The aqueous geochemistry of the rare earth elements and yttrium. Part XI. The solubility of $Nd(OH)_3$ and hydrolysis of Nd^{3+} from 30 to 290 °C at saturated water vapor pressure with in-situ pH_m measurement

SCOTT A. WOOD[1*], DONALD A. PALMER[2], DAVID J. WESOLOWSKI[2], PASCALE BÉNÉZETH[2]

[1]Department of Geological Sciences, Box 443022, University of Idaho, Moscow, ID 83844-3022
[2]Chemical and Analytical Sciences Division, Oak Ridge National Laboratory, P.O. Box 2008, Oak Ridge, TN 37831-6110

* corresponding author (swood@iron.mines.uidaho.edu)

Abstract—The solubility of well-characterized, crystalline $Nd(OH)_3(cr)$ was determined in non-complexing, 0.03-1.0 mol kg^{-1} sodium trifluoromethanesulfonate (sodium triflate, NaTr) solutions from 30° to 290 °C at saturated water vapor pressure (SWVP) over a range of pH_m (pH_m is the negative logarithm of the molal hydrogen-ion concentration). The pH_m was measured *in situ* during the solubility experiments using a hydrogen-electrode concentration cell (50°-290 °C) or a combination glass-electrode (30 °C). From 30° to 200 °C the predominant dissolved Nd species over a wide range of pH_m was found to be the aquo ion, Nd^{3+}. Over the pH_m range where Nd^{3+} predominates, the solubility of $Nd(OH)_3(cr)$ decreased strongly with increasing temperature. Stoichiometric molal equilibrium quotients (Q_{s0}) for the reaction:

$$Nd(OH)_3(cr) + 3H^+ \leftrightarrow Nd^{3+} + 3H_2O \tag{1}$$

were computed for 0.03, 0.1 and 1.0 mol kg^{-1} sodium triflate. The following equation adequately describes the measured equilibrium quotients as a function of temperature and ionic strength:

$$\log Q_{s0} = -6.662 + 7300.0/T + I(-91.51/T - 7.182 \cdot 10^{-6}T^2) - 6f^\gamma/\ln(10) - 3\log a_w$$

where T is the temperature in Kelvin, I is the ionic strength in mol kg^{-1}, a_w is the activity of water and f^γ is a Debye-Hückel term given by

$$f^\gamma = -A_\phi[x/(1 + 1.2x) + (2/1.2)\ln(1 + 1.2x)] \text{ and } x = I^{1/2}$$

From these equations we calculate $\log K_{s0} = 17.9 \pm 0.3$ at 25 °C, which compares well with a value recently derived from a critical evaluation of the pre-existing literature. We also obtain a value of $\Delta H_f^o(Nd(OH)_3(cr))$ = -1414±5 kJ mol^{-1} at 25 °C and 1 bar which is in good agreement with calorimetrically-derived values reported in the literature.

Our data also suggest that, at low temperature (30° to 100 °C), hydrolysis proceeds from Nd^{3+} to $Nd(OH)_3^0$ over a very narrow pH_m range, and intermediate species are relatively unimportant. However, at 250° and 290 °C, the $Nd(OH)^{2+}$ and $Nd(OH)_2^+$ species are significant, with the relative importance of these two species being sensitive to the ionic strength. We were able to extract stoichiometric molal equilibrium quotients at 250 and 290 °C for the reactions:

$$Nd^{3+} + H_2O(l) \leftrightarrow Nd(OH)^{2+} + H^+$$

$$Nd^{3+} + 2H_2O(l) \leftrightarrow Nd(OH)_2^+ + 2H^+$$
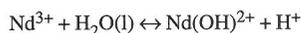
Extrapolation of these equilibrium quotients to zero ionic strength using the Debye-Hückel equation indicates that recent theoretical predictions of the first hydrolysis constant at 250° and 290 °C overestimate the degree of hydrolysis by several orders of magnitude. The solubility minimum, i.e., the region of the solubility curve where $Nd(OH)_3^0$ predominates in solution, decreases with temperature from 30° to at least 100 °C, but increases again at 290 °C. Equilibrium constants for the reaction:

$$Nd^{3+} + 3H_2O(l) \leftrightarrow Nd(OH)_3^0 + 3H^+$$

were also obtained and found to be lower than recent theoretical predictions by increasing amounts as temperature increases (more than 3 orders of magnitude lower at 290 °C).

1. INTRODUCTION

Over the last half century there have been a number of measurements of the solubility of neodymium hydroxide (Table 1) and the hydrolysis of Nd^{3+} (Table 2). Much of this work has been stimulated by the chemical similarity of Nd^{3+} to trivalent actinides (Moeller et al., 1965; Choppin, 1983, 1986, 1989; Brush, 1990; Nitsche, 1990; Millero, 1992), and the need to understand the aqueous geochemistry of the latter in order to predict their fate in the environment.

Also, this work has been driven by interest in the hydrothermal growth of single crystals of REE hydroxides owing to their magnetic, thermal and optical properties (Mroczkowski et al., 1970 and references therein). Finally, a better understanding of the thermodynamics of REE phases and aqueous species would also benefit a number of areas of geochemistry summarized by Ding and Wood (this volume) and references therein. In this paper, we are primarily concerned with the solubility product of $Nd(OH)_3(cr)$, i.e., the equilibrium constant of the reaction:

$$Nd(OH)_3(cr) + 3H^+ \leftrightarrow Nd^{3+} + 3H_2O(l) \quad (1)$$
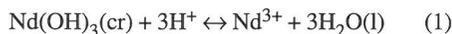
The stoichiometric molal equilibrium quotient (Q_{s0}) of the above reaction is defined as:

$$Q_{s0} = \frac{[Nd^{3+}]}{[H^+]^3} \quad (2)$$

The solubility product at infinite dilution may be written:

$$K_{s0} = \frac{a_{Nd^{3+}} a^3_{H_2O}}{a^3_{H^+}} = Q_{s0} \cdot \frac{\gamma_{Nd^{3+}} a^3_{H_2O}}{\gamma^3_{H^+}} \quad (3)$$

Table 1 shows that reported values of K_{s0} and Q_{s0} at room temperature for well-crystalline/well-aged $Nd(OH)_3$ vary over about four orders of magnitude. The solubility products for freshly precipitated/slightly aged $Nd(OH)_3$ vary over a similar range. However, as

expected, the solubility of poorly crystalline $Nd(OH)_3$ appears to be higher than that for well-crystalline $Nd(OH)_3$. Possible reasons for the discrepancies observed in Table 1 include (see also Diakonov et al., 1998): 1) differences in the crystallinity of the initial $Nd(OH)_3$; 2) partial conversion of $Nd(OH)_3$ to much less soluble hydroxycarbonates or carbonates owing to contamination of the experimental system with CO_2; 3) lack of attainment of equilibrium; 4) inaccurate pH measurement, to which K_{s0} is very sensitive owing to the fact that a_{H^+} is raised to the 3rd power (eq. 3); and 5) sampling and/or analytical uncertainties. There are very few reported values of K_{s0} for $Nd(OH)_3$ at elevated temperatures, and none above 90 °C. However, recently Deberdt et al. (1998) have determined the analogous quantities for $La(OH)_3(cr)$ and $Gd(OH)_3(cr)$ at temperatures up to 150 °C.

Hydrolysis of Nd^{3+} is described by the generalized reaction:

$$mNd^{3+} + nH_2O(l) \leftrightarrow Nd_m(OH)_n^{3m-n} + nH^+ \quad (4)$$
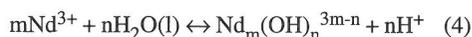
and the hydrolysis constant is given by:

$$K_{hn,m} = \frac{a_{Nd_m(OH)_n^{3m-n}} a^n_{H^+}}{a^m_{Nd^{3+}} a^n_{H_2O}} \quad (5)$$

The expression for $Q_{hn,m}$ is analogous, but is defined in terms of concentrations instead of activities, ignoring the activity of water (cf. eq. 2). Note that,

Table 1. Summary of literature data on the solubility of $Nd(OH)_3(s)$ at room temperature.

Author	T(°C)	Ionic strength and medium	log Q_{s0}
		Crystalline or well aged	
Akselrud (1963)	25	infinite dilution	18.11[1]
Spivakovskii & Moisa (1972, 1977)	25	infinite dilution	16.35[1]
Silva (1982)	25	0.1 mol L^{-1} NaClO$_4$ (extr. to 0 with Davies eq.)	16.0±0.2
Baes & Mesmer (1986)	25	infinite dilution	18.6[3]
Morss et al. (1989)	25	infinite dilution	19.7±0.7[2]
Makino et al. (1993)	22	0.01 mol L^{-1} (extr. to 0)	16.00[4]
Rao et al. (1996)	25	0.1 mol L^{-1} NaCl (extr. to 0 with Pitzer eq.)	14.96
"	90	"	14.18
Merli et al. (1997)	25	infinite dilution	17.5±0.5[2]
Diakonov et al. (1998)	25	infinite dilution	17.61[2]
This study	25	0.03 mol kg^{-1} NaTr (empirically extr. to 0)	17.9±0.3
		Fresh precipitate or slightly aged	
Moeller & Kremers (1944)	25	0.1 mol L^{-1} Nd(NO$_3$)$_3$	21.3
Moeller & Fogel (1951)	25	0.1 mol L^{-1} Nd(ClO$_4$)$_3$	20.5
Tobias & Garrett (1958)	25	0.1 mol L^{-1} HCl (extr. to 0 with Davies eq.)	18.94
Meloche & Vrátný (1959)	25	3.72 x 10^{-2} mol kg^{-1} Nd(ClO$_4$)$_3$	22.1
Orhanovic et al. (1966)	20	≤0.1 mol kg^{-1} Nd(NO$_3$)$_3$	18.1
Azhipa et al. (1967)	20	dilute HCl, LiOH	18.57[1]
Kragten & Decnop-Weever (1984)	21.5	1.0 mol L^{-1} NaClO$_4$	19.4±0.2

NOTE: Q_{s0} refers to the reaction: $Nd(OH)_3(s) + 3H^+ \leftrightarrow Nd^{3+} + 3H_2O(l)$ and is given in the same units as the ionic strength for each study. [1]Recalculated by Diakonov et al. (1998); [2]Calculated from calorimetrically-derived thermodynamic data; [3]Calculated based on a correlation with lattice parameters (see text); [4]Cited by Diakonov et al. (1998).

in equation (4), the value of m is limited to unity when the total Nd concentration is maintained at low levels by $Nd(OH)_3(cr)$ solubility (see section 4.5). It is difficult to compare the $Q_{hn,m}$ values given in Table 2 because of differences in ionic strength, etc. However, inspection of this table shows that, although the spread in measured $Q_{hn,m}$ values is generally less than that for Q_{s0}, there is some disagreement among the various measurements, and refinements are possible (see also Wood, 1990a). The clearest example is the data at 3 mol L^{-1} $NaClO_4$, for which three separate measurements of $Q_{h1,1}$ vary over an order of magnitude.

The main goal of the study reported in this paper was to determine the solubility product for $Nd(OH)_3(cr)$ as a function of temperature up to 290 °C, using in situ pH_m measurements, in the hope of resolving the discrepancies in previously reported solubility products. In addition to supplying data previously unavailable above 90 °C, the expected faster reaction kinetics at elevated temperatures should minimize uncertainties owing to a slow approach to equilibrium, which is a decided advantage in attempting to resolve the discrepancies noted above. Secondary goals were to obtain some information on the hydrolysis of Nd^{3+} at elevated temperatures, and to lay the groundwork for using measurements of the solubility of $Nd(OH)_3(cr)$ as a means of obtaining stability constants of complexes of Nd^{3+} with other ligands such as acetate, chloride or sulfate (cf. Wesolowski et al., 1998).

2. METHODS

2.1. Synthesis and Characterization of Crystalline Nd(OH)₃

Previous studies have shown that $Nd(OH)_3$ is the stable phase in the Nd-O-H system from room temperature up to roughly 800 °C (nearly independent of pressure from 200 to 2000 bars), above which it transforms to NdOOH (Viswanathiah et al., 1976; 1980). Earlier work by Shafer and Roy (1959), which suggested that $Nd(OH)_3$ was stable only to less than 450 °C, was apparently affected by contamination by CO_2, causing the formation of Nd-carbonate phases (Viswanathiah et al., 1976). The partial pressure of CO_2 at which $Nd(OH)_3$ converts to the hydroxycarbonate or carbonate phase may be as low as 10^{-6} bars (Diakonov et al., 1998), requiring that extreme caution be exercised in excluding CO_2 during synthesis and solubility measurements of the hydroxide.

Following Christensen (1966), Merli et al. (1997), and Deberdt et al. (1998), crystalline $Nd(OH)_3$ was synthesized by reacting 99.99% pure Nd_2O_3, supplied by Alfa Aesar (Lot Number P3129A), with deionized (18 MΩ-cm) water at 200-250 °C and sat-

Table 2. Summary of literature data on the hydrolysis of Nd^{3+} at room temperature.

Author	Method	T(°C)	Ionic strength and medium	Hydrolysis constants
Kragten & Decnop-Weever (1984)	Solubility	21.5	1 mol L^{-1} $NaClO_4$	log $Q_{h1,1}$ = -8.1±0.2
				log $Q_{h2,1}$ = -16.2±0.2
				log $Q_{h3,1}$ = -24.3±0.2
				log $Q_{h2,2}$ = -11.6±0.2
Silva (1982)	Solubility	25	0.1 mol L^{-1} $NaClO_4$	log $K_{h2,1}$ = -15.8±0.5
			(extr. to 0 with Davies eq.)	log $K_{h3,1}$ = -23.9±0.2
				log $K_{h4,1}$ < -34
Burkov et al. (1988)	Potentiometry	25	3 mol L^{-1} $NaClO_4$	log $Q_{h1,1}$ = -8.94±0.04
				log $Q_{h2,2}$ = -14.03±0.01
Burkov et al. (1973)	Potentiometry	25	3 mol L^{-1} $NaClO_4$	log $Q_{h1,1}$ = -9.4±0.4
				log $Q_{h2,2}$ = -13.93±0.03
Guillaumont et al. (1971)	Solvent extraction	25	0.1 mol L^{-1} $NaClO_4$	log $Q_{h1,1}$ = -7.0
Kostromina & Badaev (1986)	Spectrophotometry	25?	variable?	log $\beta_{1,1}$ = 7.4±0.4
				log $\beta_{2,2}$ = 13.0±0.7
Moeller (1946)	Potentiometry	25	0.005 mol L^{-1} $Nd_2(SO_4)_3$	log $Q_{h1,1}$ = -9.0
			0.01 mol L^{-1} $Nd_2(SO_4)_3$	log $Q_{h1,1}$ = -8.7
			0.05 mol L^{-1} $Nd_2(SO_4)_3$	log $Q_{h1,1}$ = -7.5
Tobias & Garrett (1958)	Potentiometry	25	3 mol L^{-1} $NaClO_4$	log $Q_{h1,1}$ = -8.5±0.4
Baes & Mesmer (1986)	Critical compilation	25	Infinite dilution	log $K_{h1,1}$ = -8.0
				log $K_{h2,1}$ = -16.9
				log $K_{h3,1}$ = -26.5
				log $K_{h4,1}$ = -37.1
This study	Solubility	30	0.03 mol kg^{-1} NaTr	log $Q_{h3,1}$ = -24.7±0.3

Note: $Q_{hn,m}$ ($K_{hn,m}$) refers to the reaction: $mNd^{3+} + nH_2O(l) \leftrightarrow Nd_m(OH)_n^{3m-n} + nH^+$ and is given in the same units as the ionic strength for each study; β_{nm} refers to the reaction: $mNd^{3+} + nOH^- \leftrightarrow Nd_m(OH)_n^{3m-n}$.

Table 3. Powder X-ray data for the $Nd(OH)_3(cr)$ synthesized in this study.

d(Å)	I/I_0	d(Å)	I/I_0
12.45	4	2.22	70
5.48	58	1.86	14
3.19	60	1.85	26
3.08	100	1.83	54
2.76	19	1.61	19
2.42	8	1.42	15

urated water vapor pressure in a Teflon-lined stainless steel reaction vessel for two weeks. The water was first deaerated by vigorously bubbling high-purity Ar gas through it for at least 15 minutes. Other authors (e.g., Rao et al., 1996) have synthesized the hydroxide by reacting solutions of Nd-chloride salts with aqueous hydroxide solutions, followed by aging. However, it is difficult to exclude CO_2 from aqueous hydroxide solutions. In addition, the initial products obtained by precipitating Nd from solutions of chloride salts are known to contain chloride, e.g., $Nd(OH)_2Cl$ (Spivakovskii and Moisa, 1972), and may be amorphous, requiring aging. The method of synthesis employed here eliminates interference by chloride, minimizes interference by CO_2 and results in crystalline $Nd(OH)_3$.

After synthesis, the $Nd(OH)_3$ was washed several times with deionized, deaerated water and separated

from the water by centrifugation. The solid was then dried in a vacuum oven at 50 °C and stored under Ar in a polyethylene container with a screw top. The initial Nd_2O_3 was a light blue color; this color changed to lilac upon conversion to $Nd(OH)_3$. No further changes in color were noted upon storage or at the conclusion of any solubility run. However, the grains of $Nd(OH)_3(cr)$ were observed to coarsen after experiments at ≥ 250 °C.

The solid was characterized before the solubility runs using powder X-ray diffraction (XRD), Fourier-transform infrared spectroscopy (FTIR) and thermal gravimetric analysis (TGA). After the runs the solid was characterized by XRD and FTIR. XRD analyses were conducted both at ORNL and the University of Idaho, with similar results. FTIR was conducted at ORNL using KBr pellets and a Bio-Rad FTS-60 instrument.

The results of a typical XRD analysis are given in Table 3. The d-spacings given in Table 3 are in excellent agreement with those given by Roy and McKinstry (1953) and Silva (1982) for $Nd(OH)_3(cr)$. The peaks of all XRD patterns were sharp and the background was uniformly low, consistent with well-crystallized $Nd(OH)_3$.

The application of TGA showed that weight loss upon heating occurred in three steps. A weight loss of roughly 9% occurred over the temperature range 292°-442 °C, followed by a weight loss of roughly 4.2% over the range 442°-575 °C. A much smaller, more
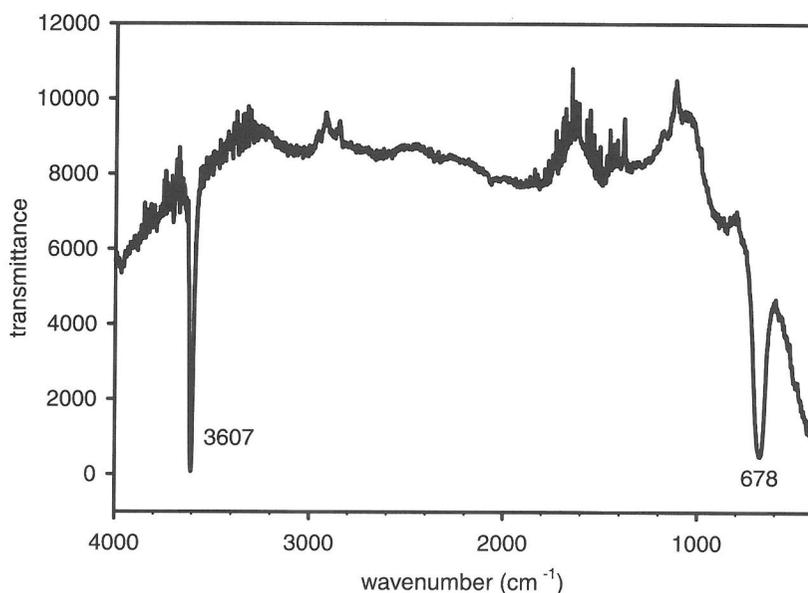

Figure 1. FTIR spectrum of $Nd(OH)_3(cr)$ synthesized in this study.

gradual weight loss of ~0.6% occurred over the range 575°-950 °C. The TGA results can be understood in terms of the following reaction:

$$2Nd(OH)_3(cr) \rightarrow Nd_2O_3(cr) + 3H_2O \qquad (6)$$
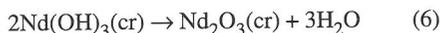
The first major step in the TGA corresponds to the loss of 2 water molecules (9.22% theoretical), and the second and third steps combined correspond to the loss of 1 water molecule (4.61% theoretical). The total measured weight loss in two separate analyses amounted to 13.80% and 14.15%, compared to the theoretical weight loss of 13.83%.

The FTIR spectrum of a sample of freshly prepared $Nd(OH)_3(cr)$ in a KBr pellet is shown in Figure 1. For this sample, all the steps in the preparation of the KBr pellet were carried out either under an Ar atmosphere in a glove box, or under vacuum. The major features of this spectrum are a sharp, intense band at 3607 cm^{-1} and a broader but intense band at 678 cm^{-1}. These features are characteristic of $Nd(OH)_3$ (Klevtsov et al., 1967), with the former and latter bands attributable to the O-H stretch and O-H bend, respectively, of hydroxide. The spectrum in Figure 1 is also notable for the absence of any significant bands between 1400 and 1500 cm^{-1}, or between 1060 and 1090 cm^{-1}, which are diagnostic of the presence of carbonate (Caro et al., 1972). However, $Nd(OH)_3$ exposed to the atmosphere for more than a few hours invariably exhibited weak bands attributable to Nd-carbonate, indicative of the difficulty in preventing the formation of these carbonates during synthesis, characterization and solubility measurements if extreme precautions are not taken to exclude CO_2.

2.2. Preparation of Solutions

All solutions were prepared by weight, employing reagent-grade chemicals and 18-MΩ-cm deionized water that had been deaerated by vigorously sparging with ultrapure argon for 15 minutes or more. The solutions were stored in polyethylene containers under positive Ar pressure. Concentrated stock solutions of NaTr, NaOH and HTr were prepared and used to make up the desired experimental solutions. The NaTr stock solution was prepared by neutralization of triflic acid with a CO_2-free, concentrated NaOH solution as described by Palmer and Hyde (1993). The compositions of the initial test, reference and titrant solutions employed in this study are given in Table 4.

2.3. Experimental Procedure
2.3.1. The hydrogen-electrode concentration cell (HECC)

Experiments from 50° to 290 °C were conducted using an HECC of the type described in several previous publications (Palmer and Wesolowski, 1993; Bénézeth et al., 1997; Wesolowski et al., 1998; Bénézeth et al., 1999; Palmer et al., 2001). The cell comprised a 1-L Hastelloy reaction vessel fitted with two concentric Teflon cups, separated by a porous Teflon liquid junction. Teflon-coated platinum wires, the ends of which were free of Teflon but coated with platinum black, were inserted into each cup and served as the electrodes. The solutions in each cup were stirred magnetically via Teflon-coated stir bars. The inner cup contained the reference solution with a

Table 4. Initial compositions (mol kg^{-1} H$_2$O) of test, reference and titrant solutions for solubility experiments.

Series	Test	Reference	Acid titrant	Basic titrant
Nd-1	$m_{H^+} = 3.085 \times 10^{-4}$ $m_{Na^+} = 2.964 \times 10^{-2}$ $m_{Tr^-} = 2.975 \times 10^{-2}$	$m_{H^+} = 1.285 \times 10^{-3}$ $m_{Na^+} = 2.858 \times 10^{-2}$ $m_{Tr^-} = 2.869 \times 10^{-2}$ $m_{Cl^-} = 9.871 \times 10^{-4}$	$m_{H^+} = 1.012 \times 10^{-2}$ $m_{Na^+} = 2.480 \times 10^{-2}$ $m_{Tr^-} = 3.492 \times 10^{-2}$	$m_{OH^-} = 9.490 \times 10^{-3}$ $m_{Na^+} = 3.321 \times 10^{-2}$ $m_{Tr^-} = 2.373 \times 10^{-2}$
Nd-2	$m_{H^+} = 3.084 \times 10^{-4}$ $m_{Na^+} = 2.943 \times 10^{-2}$ $m_{Tr^-} = 2.974 \times 10^{-2}$	$m_{H^+} = 1.142 \times 10^{-3}$ $m_{Na^+} = 2.829 \times 10^{-2}$ $m_{Tr^-} = 2.943 \times 10^{-2}$	$m_{H^+} = 3.030 \times 10^{-2}$ $m_{Na^+} = 5.103 \times 10^{-3}$ $m_{Tr^-} = 3.540 \times 10^{-2}$	$m_{OH^-} = 3.003 \times 10^{-2}$ $m_{Na^+} = 3.620 \times 10^{-2}$ $m_{Tr^-} = 6.168 \times 10^{-3}$
Nd-3	$m_{H^+} = 1.142 \times 10^{-3}$ $m_{Na^+} = 2.829 \times 10^{-2}$ $m_{Tr^-} = 2.943 \times 10^{-2}$	$m_{H^+} = 1.142 \times 10^{-3}$ $m_{Na^+} = 2.829 \times 10^{-2}$ $m_{Tr^-} = 2.943 \times 10^{-2}$	$m_{H^+} = 3.030 \times 10^{-2}$ $m_{Na^+} = 5.103 \times 10^{-3}$ $m_{Tr^-} = 3.540 \times 10^{-2}$	$m_{OH^-} = 3.003 \times 10^{-2}$ $m_{Na^+} = 3.620 \times 10^{-2}$ $m_{Tr^-} = 6.168 \times 10^{-3}$
Nd-4	$m_{H^+} = 1.040 \times 10^{-3}$ $m_{Na^+} = 9.925 \times 10^{-2}$ $m_{Tr^-} = 1.003 \times 10^{-1}$	$m_{H^+} = 1.040 \times 10^{-3}$ $m_{Na^+} = 9.925 \times 10^{-2}$ $m_{Tr^-} = 1.003 \times 10^{-1}$	None	None
Nd-5	$m_{H^+} = 1.022 \times 10^{-3}$ $m_{Na^+} = 9.757 \times 10^{-2}$ $m_{Tr^-} = 9.859 \times 10^{-2}$	$m_{H^+} = 1.040 \times 10^{-3}$ $m_{Na^+} = 9.925 \times 10^{-2}$ $m_{Tr^-} = 1.003 \times 10^{-1}$	None	$m_{OH^-} = 3.085 \times 10^{-2}$ $m_{Na^+} = 1.642 \times 10^{-1}$ $m_{Tr^-} = 1.333 \times 10^{-1}$
Nd-6	$m_{H^+} = 1.044 \times 10^{-3}$ $m_{Na^+} = 1.0063$ $m_{Tr^-} = 1.0074$	$m_{H^+} = 1.044 \times 10^{-3}$ $m_{Na^+} = 1.0063$ $m_{Tr^-} = 1.0074$	None	None

precisely known stoichiometric hydrogen-ion molality. The outer cup contained a suspension of $Nd(OH)_3(cr)$ in the test solution (initially ~10 g of solid in ~400 mL of solution). The entire HECC was purged 5-10 times with hydrogen at room temperature before being placed in the aluminum block furnace for equilibration at temperature. Upon completion of the hydrogen purge, the hydrogen pressure was set at ~10 bars at 25 °C. The initial cell configuration in a typical experiment was:

$$H_2, Pt \mid HTr\ (m_1), NaTr\ (m_2) \mid\mid HTr\ (m_3), NaTr$$
$$(m_4), Nd(OH)_3(cr) \mid Pt, H_2$$
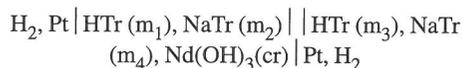
with $m_2 = m_4$ at the start of the experiment, and the ratios $m_1:m_2$ and $m_3:m_4$ maintained at less than 0.1 to minimize both liquid junction contributions to the measured potential and activity coefficient differences between the two solutions.

Samples of the test solution were withdrawn via a platinum dip tube that had a porous platinum frit gold-welded to its immersed end to prevent particles of the solid from entering the Pt tube during sampling. The portion of the Pt dip tube outside the cell was fitted with a cooling jacket, and samples were withdrawn through a PEEK® valve and a 0.2-μm fluoropolymer (PVDF) syringe filter into pre-weighed polypropylene syringes containing a known mass of high-purity 1 mol L^{-1} HNO_3 (JT Baker Ultrex Reagent). The samples were then analyzed for Nd using inductively coupled plasma-atomic emission spectroscopy (ICP-AES; Thermo Jarell Ash IRIS at ORNL) or inductively coupled plasma-mass spectrometry (ICP-MS; Perkin Elmer Elan 250 at Washington State University) depending on the Nd concentration. In initial experiments, Nd concentrations were also determined by ion chromatography. Precision of repeat analyses was normally in the range 1-10%, depending on how close the Nd concentration was to the detection limit of the analytical technique employed. There was excellent agreement among analytical techniques where analytical working ranges overlapped.

Upon attainment of equilibrium (usually within a day or two; see below for the criteria applied to define attainment of equilibrium), a small amount of either NaOH + NaTr or HTr + NaTr titrant solution at the same ionic strength as the reference and test solutions was injected into the test cell using one of two calibrated positive displacement pumps (Zircadyne 705) to change the pH_m. After equilibrium was reestablished, another sample was taken for total Nd determination. This stepwise process was repeated until a portion of the Nd-hydroxide solubility curve as a function of pH_m was mapped out. Use of two inert, positive-displacement pumps permitted us to reverse

the solution titration process and approach equilibrium from both under- and over-saturation.

The working definition of pH_m throughout this paper is $pH_m = -\log\ [H^+]$, where $[H^+]$ is the hydrogen-ion concentration in mol kg^{-1} units. The convention employed is that triflic acid and NaOH are completely dissociated, and NaTr ion-pairing is treated implicitly by the activity coefficient model used.

Each platinum-hydrogen electrode responds to the half-cell reaction:

$$H_2(g) \leftrightarrow 2H^+ + 2e^- \tag{7}$$
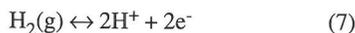
and the difference in potential between the two electrodes is given by the Nernst equation:

$$\Delta E = -\frac{RT}{F}\ln([H^+]_t/[H^+]_r) - E_{LJ} \tag{8}$$

where $[H^+]_t$ and $[H^+]_r$ represent the stoichiometric molalities of hydrogen ion in the test and reference solutions, respectively. The ideal gas and Faraday constants are R and F, respectively, and T is the temperature in Kelvin. Finally, E_{LJ} represents the liquid junction potential calculated using the Henderson equation (Baes and Mesmer, 1986). The limiting equivalent conductances of ions required by the Henderson equation were taken from the following sources: Na$^+$, H$^+$ and OH$^-$ (Quist and Marshall, 1965) and Tr$^-$ (Ho and Palmer, 1995). The limiting equivalent conductances of Nd^{3+} were approximated with those of La^{3+}, which are available only from 0 to 100 °C (Robinson and Stokes, 1959), and therefore were extrapolated to higher temperatures. The maximum liquid junction potential calculated in this study was 20 mV, which contributes an uncertainty of <±0.1 in the measured pH_m, assuming that the Henderson equation predicts the value of E_{LJ} to within 25% (Mesmer, 1991). However, the only conditions for which such high values of E_{LJ} were calculated were those where pH_m was sufficiently low at any given temperature that Nd^{3+} accounted for a significant fraction of the ions present in the test compartment. This only occurred at the lowest ionic strength investigated, i.e., 0.03 mol kg^{-1} NaTr, and then only for the most acidic conditions. For most of the data points at 0.03 mol kg^{-1} NaTr, the maximum calculated E_{LJ} was <6 mV, contributing an uncertainty in the measured pH_m of <±0.025. At 0.1 and 1.0 mol kg^{-1} NaTr, the maximum calculated values of E_{LJ} were 2 mV and 0.1 mV, respectively. These contribute uncertainties of <±0.01 and <±0.0005 in the measured pH_m.

### 2.3.2. Glass-electrode cell

Solubility experiments at 30 °C were conducted in a 500-mL polystyrene bottle. The temperature was

maintained constant to within ±0.1 °C using a water bath. The bottle was fitted with a combination glass pH electrode and tubing to maintain a positive-pressure Ar atmosphere. The electrode was calibrated at 30 °C against three to five solutions containing known, stoichiometric amounts of HTr or NaOH and sufficient NaTr to make the total ionic strength identical to that of the solubility experiment (i.e., 0.03 molal). Samples were withdrawn via a syringe and immediately filtered through a 0.2-μm fluoropolymer membrane into pre-weighed polypropylene syringes containing a known mass of high-purity 1 mol L^{-1} HNO$_3$ (JT Baker Ultrex Reagent). The samples were analyzed as described above. After equilibrium was attained at a given pH$_m$ value, a known quantity of acid or base was titrated into the bottle to shift the pH$_m$ and the entire process was repeated.

2.4. Data Reduction
2.4.1. Determination of stoichiometric molal equilibrium quotients

If polynuclear species are neglected, then the solubility of Nd(OH)$_3$(cr) as a function of pH$_m$ can be expressed in terms of the generalized dissolution reaction:

$$Nd(OH)_3(cr) + (3-n)H^+ \leftrightarrow$$
$$Nd(OH)_n^{3-n} + (3-n)H_2O \qquad (9)$$
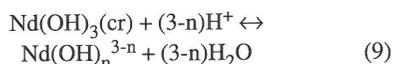
for which the conditional equilibrium constant can be written as:

$$Q_{sn} = \frac{[Nd(OH)_n^{3-n}]}{[H^+]^{3-n}} \qquad (10)$$

Taking the log of both sides of equation (10) and rearranging yields:

$$\log[Nd(OH)_n^{3-n}] = \log Q_{sn} - (3-n)pH_m \qquad (11)$$

Now, differentiating the concentration of the Nd species with respect to pH$_m$ we obtain:

$$\frac{\partial \log[\Sigma Nd]}{\partial pH_m} = n - 3 \qquad (12)$$

Thus, from equations (11) and (12), we see that the slope of a plot of log [ΣNd] vs. pH$_m$ at any point yields the value of n-3. If any one species is predominant over a wide range of pH$_m$, then the solubility curve over that pH$_m$ range should approximate a straight line with slope n-3, where n is the number of hydroxide ions bound to the Nd^{3+} ion in the predominant species.

The total measured Nd concentration in solution can be expressed as:

$$[\Sigma Nd] = [Nd^{3+}] + [NdOH^{2+}] + [Nd(OH)_2^+] +$$

$$[Nd(OH)_3^0] + \ldots + [Nd(OH)_N^{3-N}] \qquad (13)$$

where N is the maximum hydroxide ligand number. Expressing the concentrations of each of the Nd species in terms of its corresponding Q$_{sn}$ value we obtain:

$$[\Sigma Nd] = Q_{s0} \cdot [H^+]^3 + Q_{s1} \cdot [H^+]^2 + Q_{s2} \cdot [H^+]^1 +$$
$$Q_{s3} + \ldots Q_{sN} \cdot [H^+]^{3-N} \qquad (14)$$

This equation can be fit to a set of experimental data for the solubility of Nd(OH)$_3$(cr) as a function of pH$_m$, at a constant ionic strength and temperature, using non-linear regression, to obtain the values of Q$_{sn}$ as fit coefficients. The best fit model is the one containing the fewest species while minimizing the function:

$$\sqrt{\frac{\sum_{i=1}^{p} \left(\log[\Sigma Nd]_{obs} - \log[\Sigma Nd]_{calc} \right)^2}{p-q}} \qquad (15)$$

where p is the total number of solubility measurements and q (= N + 1) is the number of species in the model. In this study, non-linear regression was performed using the least-squares routine in the software package SigmaPlot® (Jandel Scientific), which employs the Marquardt-Levenberg algorithm, and also using a version of the generalized regression program ORGLS (Busing and Levy, 1962). Results obtained using the two regression algorithm were essentially identical.

As will be shown below, for most combinations of temperature and ionic strength, only a single species, the hydrated Nd^{3+} ion, predominated over a wide range of pH$_m$. In these cases, regression was unnecessary because only one parameter, Q$_{s0}$, was required to fit the data. In these cases, an estimate of Q$_{s0}$ was calculated for each data point as:

$$Q_{s0} = \frac{[\Sigma Nd]}{[H^+]^3} \qquad (16)$$

The accepted value of Q$_{s0}$ was then the average of all the Q$_{s0}$ values calculated according to equation (16) at a given temperature and ionic strength.

Once values of Q$_{sn}$ were determined, then the stoichiometric molal equilibrium quotients (Q$_{hn,1}$) for the hydrolysis reaction (eq. 4) were calculated according to the relation:

$$\log Q_{hn,1} = \log Q_{sn} - \log Q_{s0} \qquad (17)$$

2.4.2. Extrapolation to infinite dilution

Values of Q$_{s0}$ were obtained over a sufficient range of ionic strength at each temperature to employ an empirical method of extrapolation to zero
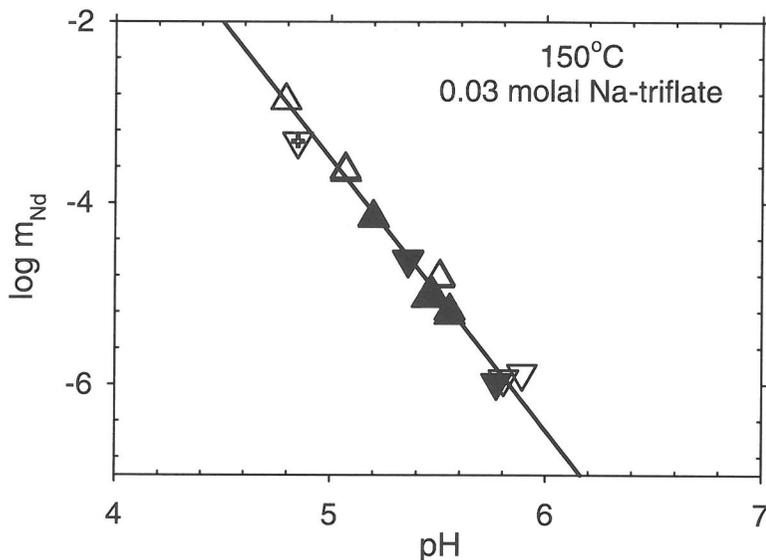
Figure 2. Plot of log $m_{\Sigma Nd}$ vs. pH_m at 150 °C and 0.03 mol kg^{-1} ionic strength demonstrating the reversibility of the solubility equilibrium. Upward-pointing and downward-pointing triangles correspond to approach from undersaturation and oversaturation, respectively. The three different styles of triangles (open, closed, open with cross) represent three separate experimental runs and illustrate the excellent reproducibility of the experimental data. The solid line represents the best fit line through the data with slope constrained at 3.0.

ionic strength. The following function of ionic strength and temperature was fit to the entire set of values of Q_{s0}:

$$\log Q_{s0} = a + b/T + I(c/T + dT^2) - 6f^\gamma/\ln(10) - 3\log a_w \qquad (18)$$

The fourth term in the equation is the Debye-Hückel expression used in the Pitzer ion-interaction model (Pitzer et al., 1977) with

$$f^\gamma = -A_\phi[x/(1 + 1.2x) + (2/1.2)\ln(1 + 1.2x)]$$
$$\text{where } x = I^{1/2} \qquad (19)$$

In the fourth term, the coefficient -6 is equal to the change in the charges squared for reaction (1). The parameter A_ϕ is the Debye-Hückel osmotic coefficient parameter for water, obtained from the temperature function given by Dickson et al. (1990). The activity of water (a_w) was calculated from the osmotic coefficients for water in NaCl solutions given by Liu and Lindsay (1972), assuming that the activity of water is the same for NaCl and NaTr solutions of equal ionic strength. In equation (18), a,b,c and d are fit parameters determined by regression using ORGLS.

Most other equilibrium quotients were obtained only at a single ionic strength (0.03 or 0.1 mol kg^{-1}). Therefore, these constants were extrapolated to infinite dilution using the Debye-Hückel equation:

$$\log \gamma_i = \frac{-A_\gamma |Z_i^2| I^{1/2}}{1 + B_\gamma \mathring{a} I^{1/2}} \qquad (20)$$

The A_γ and B_γ values employed in conjunction with equation (20) were taken from Helgeson and Kirkham (1974).

3. RESULTS

The results of the solubility experiments are given in Appendices I (30 °C) and II (50°-290°C). Gaps in the sequence of sample numbers correspond to samples obtained when the magnetic stirrer was not functioning properly and such data were not included in the data reduction.

3.1. Attainment of Equilibrium

The approach to equilibrium could be monitored by observing the rate of change of pH_m of the test solution (which is proportional to the continuously displayed cell potential). In general, samples were not withdrawn from the cell until the cell potential reached a plateau as a function of time. A lack of change of pH_m with time is a necessary, but not sufficient, criterion for the attainment of equilibrium. However, as mentioned above, the use of two positive
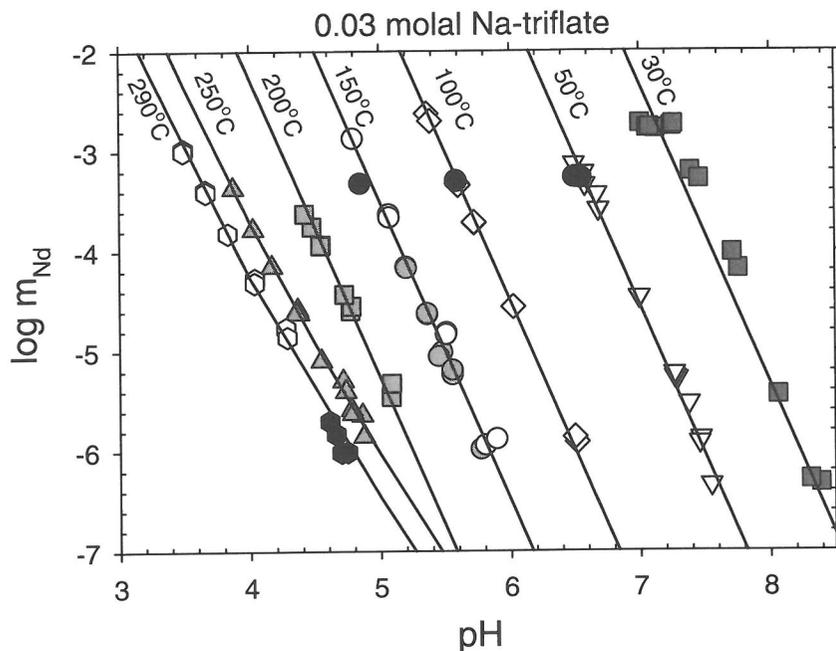
Figure 3. Plot of log $m_{\Sigma Nd}$ vs. pH_m at 0.03 mol kg^{-1} ionic and various temperatures. The four different symbol shadings (none, light gray, dark gray, black) correspond to four separate experimental runs and illustrate the excellent reproducibility of the experimental data. For temperatures 30°-200 °C, the solid lines correspond to a best fit assuming Nd^{3+} is the only Nd species present and have a constant slope of 3.0. At 250° and 290 °C, the solid curves correspond to a best fit assuming Nd^{3+} and $Nd(OH)^{2+}$ are the only species present.

displacement pumps, one to deliver acid and one to deliver base, permitted us to reverse the solubility equilibrium. The data in Figure 2 demonstrate this reversal procedure for 150 °C and 0.03 molal Na-triflate. In the figure, upward-pointing triangles denote approach to equilibrium from undersaturation, whereas downward-pointing triangles denote approach from oversaturation. The three different types of triangles represent three separate runs with three separate batches of $Nd(OH)_3$(cr). Successive samples during each run were taken at approximately half-day to day intervals (see Appendix II). Figure 2 demonstrates the excellent reproducibility of the data from run to run, and the solid triangles in particular demonstrate that the solubility reaction is readily reversible. These data suggest that equilibrium was closely attained within a day at 150 °C. Similar experiments showed that it took up to 1-3 days to equilibrate at 50-100 °C, but only a few hours at temperatures near 250-290 °C.

It is clear that the efficient agitation provided by the Teflon-coated magnetic stir bar was essential to the relatively rapid approach to equilibrium. On a number of occasions during this study, the magnetic stirrer failed, either because the motor stopped (the brushes required replacement) or the coupling between the motor and the external magnet broke. Data obtained during brief periods in which the stirrer was not functioning were neither reproducible nor reversible, and were discarded. These findings are in agreement with those of Bénézeth et al. (1997, 2001) and Palmer et al. (2001), who noted that equilibration rates were also rapid for the dissolution of boehmite with the efficient stirring in the HECC.

3.2. Temperature and Ionic Strength Dependence of Q_{s0}

The data obtained in 0.03 mol kg^{-1} Na-triflate as a function of temperature are shown in Figure 3. This figure demonstrates a number of features. First, the data at each temperature are quite reproducible from run to run. Second, the data from 30° to 200 °C, inclusive, plot along straight lines of slope equal to -3.0, indicating that, over the pH_m ranges shown, the predominant species in solution is the hydrated cation, Nd^{3+}. The data at 250° and 290 °C can be explained by a two-species model, the details of which are discussed below. Third, the solubility of $Nd(OH)_3$(cr) is

markedly retrograde, i.e., decreases strongly with temperature. Finally, it can be seen that the data for 30 °C scatter more strongly about a line with slope -3.0 than the data for other temperatures. This behavior is probably explained by: 1) the greater drift and difficulty in calibrating glass electrodes compared to hydrogen electrodes; 2) slower rates of equilibration at the lower temperatures.

Values of $\log Q_{s0}$ for 0.03 mol kg^{-1} Na-triflate were derived from the data from 30° to 250 °C as described in section 2.4.1. From 30° to 200 °C, inclusive, only one species appears to be present over the entire pH_m range shown in Figure 3, and Q_{s0} is reported as the average of values calculated from equation (16). At 250 °C and 0.03 mol kg^{-1} NaTr, two species were apparently present over the range of pH_m shown in Figure 3, and Q_{s0} was obtained using non-linear regression as described in section 2.4.1. The values of Q_{s0} at 250 °C and 0.1 and 1.0 mol kg^{-1} ionic strengths were calculated assuming that Nd^{3+} was the predominant species at the relatively low pH_m (~4) of the solubility measurements made. This is a reasonable assumption because at 0.03 mol kg^{-1} ionic strength and 250 °C Nd^{3+} is predominant at similar values of pH_m, and higher ionic strength should favor the most highly charged species. At 290 °C, Nd^{3+} was not predominant over a sufficiently large range of investigated pH_m at either 0.03 or 0.1 mol kg^{-1} ionic strength, and so no Q_{s0} values were derived from the data at 290 °C. No solubility measurements were obtained at 290 °C and 1.0 mol kg^{-1} ionic strength.

The raw values of Q_{s0} obtained in this study are compiled in Table 5. The values of Q_{s0} at 0.03 mol kg^{-1} ionic strength are plotted as a function of inverse temperature in Figure 4. The plot of $\log Q_{s0}$ vs. $1/T$ is highly linear from 30° to 250 °C. Thus, it appears that the change in the heat capacity of reaction (1) is near zero. Equation (18) was fit to the entire data set given in Table 5 to obtain the following expression:

Table 5. Stoichiometric molal equilibrium quotients ($\log Q_{s0}$) determined in this study as a function of temperature and ionic strength.

T(°C)	I (mol kg^{-1})	$\log Q_{s0}$	T(°C)	I (mol kg^{-1})	$\log Q_{s0}$
30	0.03	18.6±0.6	50	0.10	16.68±0.14
50	0.03	16.49±0.16	100	0.10	13.79±0.10
50	0.03	16.32±0.16	150	0.10	11.59±0.10
100	0.03	13.54±0.24	200	0.10	9.88±0.10
100	0.03	13.46±0.10	250	0.10	8.53±0.10
150	0.03	11.42±0.12	50	1.0	16.82±0.10
150	0.03	11.22±0.10	100	1.0	13.93±0.10
150	0.03	11.65±0.13	150	1.0	11.72±0.10
200	0.03	9.74±0.18	200	1.0	9.98±0.10
250	0.03	8.04±0.16	250	1.0	8.60±0.10

$$\log Q_{s0} = -5.696 + 7218/T$$
$$r^2 = 0.9946$$

I = 0.03 molal

Figure 4. Plot of $\log Q_{s0}$ vs. $1/T(K)$ for reaction (1) at 0.03 mol kg^{-1} ionic strength.

Table 6. Smoothed stoichiometric molal equilibrium quotients (log Q_{s0})
and thermodynamic properties for reaction (1) as a function of temperature and ionic strength.

T(°C)	log Q_{s0}	$\Delta G_r°$ (kJ mol^{-1})	$\Delta H_r°$ (kJ mol^{-1})	$\Delta S_r°$ (kJ mol^{-1} K^{-1})	$\Delta C_{p,r}°$ (kJ mol^{-1} K^{-1})
			$I = 0$ mol kg^1		
0	20.17±0.35	-105.5±1.8	-140.3±5.2	-0.13±0.01	0.00±0.00
25	17.92±0.27	-102.3±1.5	-140.3±5.2	-0.13±0.01	0.00±0.00
50	16.02±0.20	-99.1±1.3	-140.3±5.2	-0.13±0.01	0.00±0.00
75	14.39±0.16	-95.9±1.0	-140.3±5.2	-0.13±0.01	0.00±0.00
100	12.98±0.12	-92.7±0.9	-140.3±5.2	-0.13±0.01	0.00±0.00
125	11.75±0.10	-89.6±0.8	-140.3±5.2	-0.13±0.01	0.00±0.00
150	10.66±0.10	-86.4±0.8	-140.3±5.2	-0.13±0.01	0.00±0.00
175	9.70±0.12	-83.2±1.0	-140.3±5.2	-0.13±0.01	0.00±0.00
200	8.83±0.14	-80.0±1.2	-140.3±5.2	-0.13±0.01	0.00±0.00
225	8.05±0.16	-76.8±1.5	-140.3±5.2	-0.13±0.01	0.00±0.00
250	7.35±0.18	-73.6±1.8	-140.3±5.2	-0.13±0.01	0.00±0.00
275	6.71±0.20	-70.4±2.1	-140.3±5.2	-0.13±0.01	0.00±0.00
300	6.13±0.22	-67.2±2.4	-140.3±5.2	-0.13±0.01	0.00±0.00
			$I = 0.03$ mol kg^1		
0	20.60±0.34	-107.7±1.8	-140.5±5.1	-0.12±0.01	0.00±0.00
25	18.36±0.26	-104.8±1.5	-140.5±5.1	-0.12±0.01	0.00±0.00
50	16.48±0.20	-102.0±1.2	-140.6±5.1	-0.12±0.01	0.00±0.00
75	14.88±0.15	-99.2±1.0	-140.6±5.1	-0.12±0.01	0.00±0.00
100	13.50±0.12	-96.4±0.8	-140.7±5.1	-0.12±0.01	0.00±0.00
125	12.30±0.10	-93.7±0.8	-140.8±5.1	-0.12±0.01	0.00±0.00
150	11.25±0.10	-91.1±0.8	-140.9±5.1	-0.12±0.01	0.00±0.00
175	10.33±0.11	-88.6±1.0	-141.0±5.0	-0.12±0.01	-0.01±0.00
200	9.52±0.13	-86.2±1.2	-141.2±5.0	-0.12±0.01	-0.01±0.00
225	8.81±0.15	-84.0±1.4	-141.3±5.0	-0.12±0.01	-0.01±0.00
250	8.19±0.17	-82.0±1.7	-141.5±5.0	-0.11±0.01	-0.01±0.00
275	7.65±0.19	-80.3±2.0	-141.6±4.9	-0.11±0.01	-0.01±0.00
300	7.20±0.21	-79.0±2.3	-141.8±4.9	-0.11±0.01	-0.01±0.00
			$I = 0.1$ mol kg^1		
0	20.84±0.32	-109.0±1.7	-140.7±4.9	-0.12±0.01	-0.01±0.00
25	18.61±0.25	-106.2±1.4	-140.9±4.9	-0.12±0.01	-0.01±0.00
50	16.74±0.19	-103.6±1.2	-141.1±4.9	-0.12±0.01	-0.01±0.00
75	15.15±0.14	-101.0±0.9	-141.3±4.8	-0.12±0.01	-0.01±0.00
100	13.78±0.11	-98.4±0.8	-141.6±4.8	-0.12±0.01	-0.01±0.00
125	12.60±0.09	-96.0±0.7	-141.9±4.7	-0.12±0.01	-0.01±0.00
150	11.57±0.09	-93.7±0.8	-142.2±4.7	-0.12±0.01	-0.02±0.00
175	10.68±0.11	-91.6±0.9	-142.6±4.6	-0.11±0.01	-0.02±0.00
200	9.90±0.12	-89.6±1.1	-143.1±4.6	-0.11±0.01	-0.02±0.01
225	9.22±0.14	-87.9±1.3	-143.6±4.5	-0.11±0.01	-0.02±0.01
250	8.64±0.16	-86.6±1.6	-144.1±4.4	-0.11±0.01	-0.02±0.01
275	8.16±0.17	-85.7±1.8	-144.7±4.3	-0.11±0.01	-0.03±0.01
300	7.79±0.19	-85.5±2.1	-145.4±4.2	-0.10±0.01	-0.03±0.01
			$I = 0.3$ mol kg^1		
0	21.08±0.28	-110.2±1.5	-141.5±4.4	-0.11±0.01	-0.02±0.01
25	18.85±0.21	-107.6±1.2	-142.0±4.4	-0.12±0.01	-0.02±0.01
50	16.98±0.16	-105.0±1.0	-142.6±4.3	-0.12±0.01	-0.03±0.01
75	15.39±0.12	-102.6±0.8	-143.3±4.2	-0.12±0.01	-0.03±0.01
100	14.03±0.09	-100.2±0.7	-144.1±4.1	-0.12±0.01	-0.04±0.01
125	12.86±0.08	-98.0±0.6	-145.0±4.0	-0.12±0.01	-0.04±0.01
150	11.84±0.08	-95.9±0.7	-146.1±3.9	-0.12±0.01	-0.05±0.01
175	10.96±0.09	-94.1±0.8	-147.3±3.8	-0.12±0.01	-0.050.01
200	10.21±0.10	-92.4±0.9	-148.6±3.8	-0.12±0.01	-0.06±0.02
225	9.56±0.12	-91.2±1.1	-150.1±3.8	-0.12±0.01	-0.06±0.02

(continues)

(Table 6. continued)

250	9.02±0.13	-90.4±1.3	-151.7±3.8	-0.12±0.01	-0.07±0.02
275	8.60±0.15	-90.2±1.5	-153.5±3.8	-0.12±0.01	-0.08±0.02
300	8.31±0.16	-91.2±1.7	-155.5±4.0	-0.11±0.01	-0.08±0.02
		$I = 1.0$ mol kg^1			
0	21.08±0.32	-110.2±1.7	-144.1±3.9	-0.12±0.01	-0.06±0.02
25	18.83±0.27	-107.5±1.5	-145.8±3.9	-0.13±0.01	-0.07±0.02
50	16.92±0.22	-104.7±1.4	-147.8±4.1	-0.13±0.01	-0.09±0.02
75	15.30±0.18	-102.0±1.2	-150.2±4.4	-0.14±0.01	-0.10±0.03
100	13.90±0.15	-99.3±1.1	-152.9±4.8	-0.14±0.01	-0.12±0.03
125	12.69±0.13	-96.8±1.0	-156.0±5.3	-0.15±0.01	-0.13±0.04
150	11.64±0.12	-94.3±1.0	-159.5±6.0	-0.15±0.01	-0.15±0.04
175	10.73±0.13	-92.0±1.1	-163.5±6.8	-0.16±0.02	-0.17±0.04
200	9.94±0.15	-90.0±1.4	-167.9±7.8	-0.17±0.02	-0.19±0.05
225	9.27±0.18	-88.4±1.7	-172.8±8.9	-0.17±0.02	-0.21±0.06
250	8.72±0.22	-87.3±2.2	-178.3±10.3	-0.17±0.02	-0.23±0.06
275	8.30±0.26	-87.1±2.7	-184.4±11.7	-0.18±0.03	-0.26±0.07
300	8.06±0.31	-88.5±3.4	-191.1±13.4	-0.18±0.03	-0.28±0.07

$$\log Q_{s0} = -6.662 + 7300.0/T + I(-91.51/T - 7.182 \cdot 10^{-6}T^2) - 6f^\gamma/\ln(10) - 3\log a_w \quad (21)$$

Figure 5 shows that equation (21) provides an excellent fit to all the data except that for 30 °C and 0.03 mol kg^{-1} (see section 4.1). Smoothed values of Q_{s0}, together with thermodynamic quantities for reaction (1), i.e., ΔG_r°, ΔH_r°, ΔS_r°, and $\Delta C_{p,r}^\circ$, were calculated based on equation (21) and are given at infinite dilution and several discrete ionic strengths in Table 6.

3.3. Hydrolysis of Nd^{3+}

Our data for Nd^{3+} hydrolysis are more limited than our data for Q_{s0}. Nevertheless, we can draw a number of preliminary conclusions. Figure 6 shows
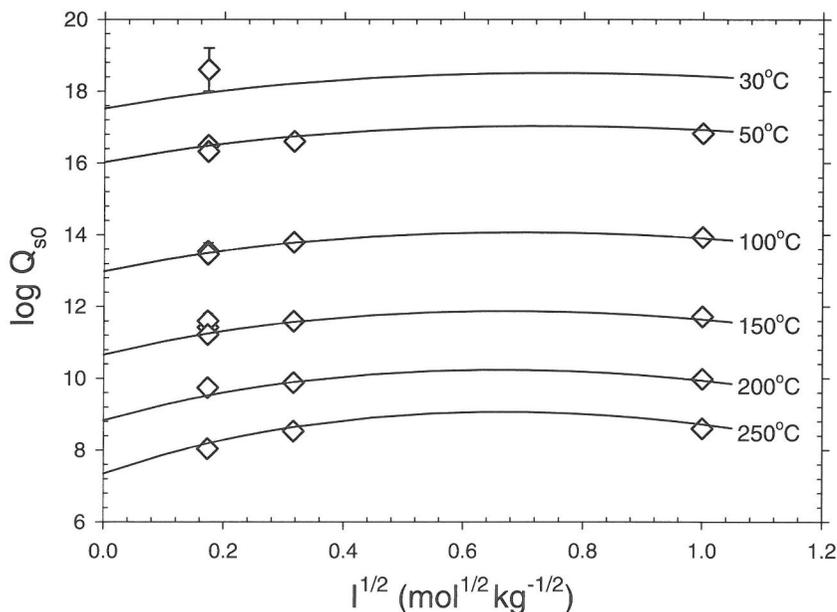

Figure 5. Plot of log Q_{s0} vs. $I^{1/2}$ for reaction (1) at various temperatures. Curves represent best fit of equation (21) in text to the data.
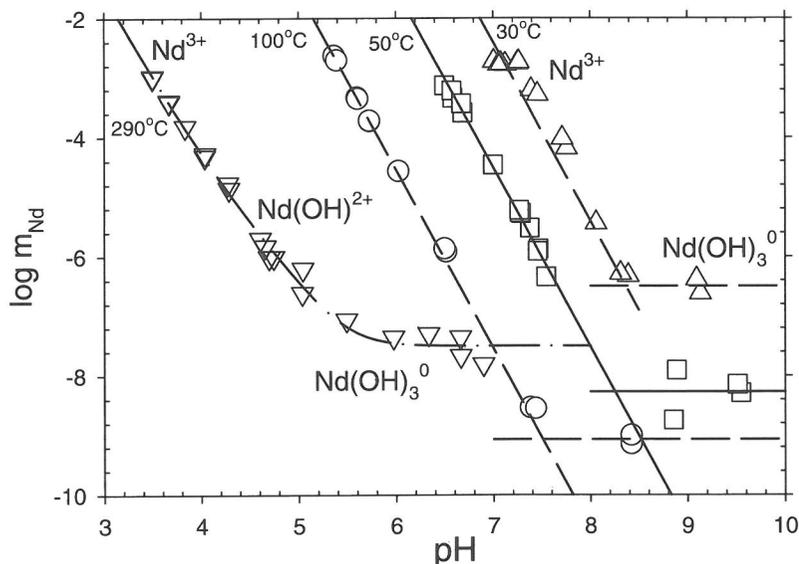
Figure 6. Plot of log $m_{\Sigma Nd}$ vs. pH_m at 0.03 mol kg^{-1} ionic and various temperatures showing the solubility minima. Note that each set of data at 30, 50 and 100 °C can be fit adequately by two straight lines of slopes –3 and 0, suggesting that Nd^{3+} and $Nd(OH)_3^0$ are the predominant species. Three species are required to fit the data at 290 °C.

that, at 30°, 50° and 100 °C, hydrolysis appears to proceed from Nd^{3+} to $Nd(OH)_3^0$ over a very narrow interval of pH_m. It therefore appears that intermediate hydrolysis products such as $Nd(OH)^{2+}$ and $Nd(OH)_2^+$ are not of great importance at the lower temperatures of these experiments. This is consistent with the conclusion of Baes and Mesmer (1986), based on a review of the literature, that the transition from aqueous REE^{3+} to $REE(OH)_3^0$ occurs over a very narrow pH range, and with the behavior of aluminum (Wesolowski and Palmer, 1994). The lack of a significant region of predominance at low temperatures for $Nd(OH)^{2+}$ and $Nd(OH)_2^+$ over the range of ionic strengths investigated in this study also is shown clearly in the work of Silva (1982) (his Fig. 9) at 0.1 mol L^{-1} NaClO$_4$ and Kragten and Decnop-Weever (1984) (their Fig. 1) at 1 mol L^{-1} NaClO$_4$. Values of Q_{s3}, i.e., the equilibrium constant for the reaction:

$$Nd(OH)_3(cr) \leftrightarrow Nd(OH)_3^0 \qquad (22)$$

at 30°, 50° and 100 °C, were determined by averaging the data at the solubility minimum at each temperature.

However, at higher temperatures, intermediate hydrolysis products appear to become more important. As shown in Figures 3 and 6, at 250° and 290 °C, there appears to be a substantial pH_m range where the slope of the solubility curve is neither –3 nor zero. Figure 7 shows that, at 290 °C and 0.03 mol kg^{-1} NaTr, a model involving the species: Nd^{3+},

$Nd(OH)^{2+}$ and $Nd(OH)_3^0$ provides a better fit to the data than a model involving the species: Nd^{3+}, $Nd(OH)^{2+}$ and $Nd(OH)_2^+$. In fact, $Nd(OH)^{2+}$ is the predominant species over a substantial pH_m range. Note that in both fits, the contribution of Nd^{3+} was estimated from the value of Q_{s0} extrapolated assuming that equation (21) is valid to at least 290 °C (an extrapolation of 40 °C); the contribution of Nd^{3+} to the measured solubility data is insufficient to permit the direct derivation of Q_{s0} from a regression of the data. The equilibrium constants for $Nd(OH)^{2+}$ and $Nd(OH)_3^0$, i.e., Q_{s1} and Q_{s3}, respectively, were obtained from non-linear regression of the data shown in Figure 7 after subtracting the minor contribution of Nd^{3+} to the total solubility. The curve fitted to the solubility data at 250 °C and 0.03 mol kg^{-1} ionic strength given in Figure 3 was obtained by regressing the data simultaneously with a model including both Nd^{3+} and $Nd(OH)^{2+}$, and it is obvious that such a model fits the data well. The experiments at 250 °C did not extend to sufficiently high pH_m to be able to detect further hydrolysis products, i.e., $Nd(OH)_3^0$.

The data at 290 °C and 0.1 molal ionic strength also demonstrate the existence of species in addition to Nd^{3+} and $Nd(OH)_3^0$ (Figure 8). In order to model the solubility data at these conditions, the contribution of Nd^{3+} was estimated from log Q_{s0} = 7.92±0.2 obtained from equation (21). The contribution of $Nd(OH)_3^0$ was estimated by noting that reaction (22) does not in-
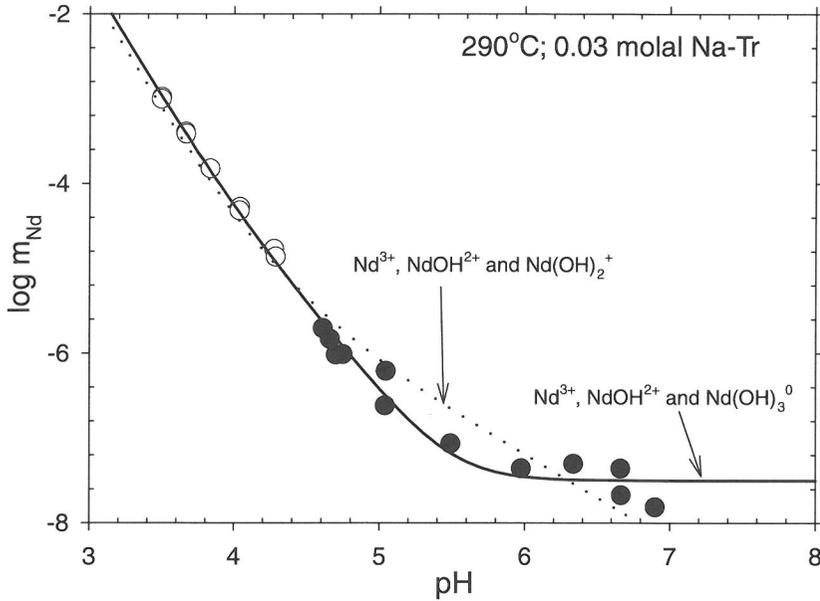
Figure 7. Plot of log $m_{\Sigma Nd}$ vs. pH_m at 0.03 mol kg^{-1} ionic strength and 290 °C showing the fit of two different speciation models. The solid line corresponds to a model including Nd^{3+}, $NdOH^{2+}$ and $Nd(OH)_3^0$; the dotted line corresponds to a model including Nd^{3+}, $NdOH^{2+}$ and $Nd(OH)_2^+$. The open and closed circles represent data obtained using ICP-AES and ICP-MS, respectively.
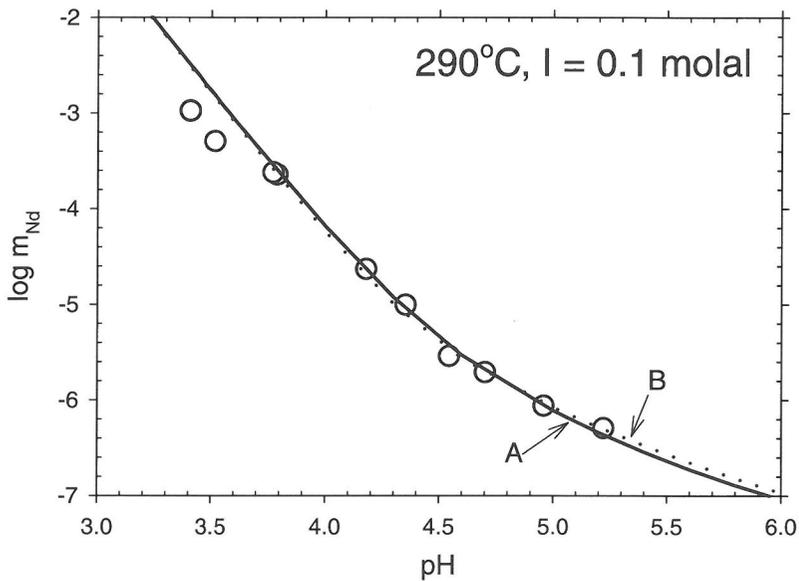
Figure 8. Plot of log $m_{\Sigma Nd}$ vs. pH_m at 0.1 mol kg^{-1} ionic strength and 290 °C showing two speciation models including Nd^{3+}, $NdOH^{2+}$, $Nd(OH)_2^+$ and $Nd(OH)_3^0$. The solid line is the fit provided by model A: log Q_{s0} = 7.7; log Q_{s1} = 3.0; log Q_{s2} = -1.23; log Q_{s3} = -7.50. The dotted line is the model B fit: log Q_{s0} = 7.7; log Q_{s1} = -4.997; log Q_{s2} = -1.12; log Q_{s3} = -7.50.

Table 7. Stoichiometric molal equilibrium quotients for the formation of hydrolyzed species.

T(°C)	I (mol kg^{-1})	n	log Q_{sn}	T(°C)	I (mol kg^{-1})	n	log Q_{sn}
30	0.03	3	-6.5±0.2	290	0.1	2	-1.3±0.2
50	0.03	3	-8.3±0.4	250	0.03	1	3.92±0.04
100	0.03	3	-9.1±0.1	290	0.03	1	3.5±0.1
290	0.03	3	-7.5±0.1	290	0.1	1	≤3.0±0.3

volve any charged species, and therefore Q_{s3} should not be highly dependent on ionic strength. Thus, the value of Q_{s3} determined at 0.03 mol kg^{-1} ionic strength, i.e., log Q_{s3} = -7.50±0.1 was assumed to be valid also at 0.1 mol kg^{-1}. It was determined that use of log Q_{s0} = 7.92±0.2 resulted in the overestimation of the solubility data at low pH, so this value was adjusted to 7.7, which provides a better fit to the data in Figure 8 and is within the uncertainty range given. Thus, log Q_{s0} and log Q_{s3} were fixed at 7.7 and –7.5, respectively, and Q_{s1} and Q_{s2} were obtained by regression. This procedure resulted in curve B in Figure 8, and the values log Q_{s1} = -5.0 and log Q_{s2} = -1.12±0.2. Moreover, the error in the estimate of Q_{s1} given by SigmaPlot was many orders of magnitude larger than Q_{s1}, which suggests that this equilibrium quotient cannot be resolved from the data shown in Figure 8. Next, Q_{s1} was fixed at various values and Q_{s2} was obtained by regression. The value of Q_{s2} obtained was not very sensitive to the value of Q_{s1} selected. Curve A in Figure 8 shows the fit of a model where log Q_{s1} was fixed at 3.0 and log Q_{s2} was refined to a value of –1.23. It is evident that there is very little difference between the fits provided by curves A and B. However, if log Q_{s1} was fixed at a value significantly above 3.0, the fit was degraded significantly. In light of these results, we can really only place an upper limit of 3.0 on the value of log Q_{s1}. The results of the calculations of Q_{s1}, Q_{s2} and Q_{s3} are given in Table 7.

Our results suggest that the relative importance of $Nd(OH)^{2+}$ and $Nd(OH)_2^+$ is quite sensitive to ionic strength at 290 °C. At 0.03 mol kg^{-1} NaTr, $Nd(OH)_2^+$ never appears to be predominant, but $Nd(OH)^{2+}$ exhibits a substantial pH range of predominance. The situation is reversed at 0.1 mol kg^{-1} NaTr. The greater importance of the lower charge species at higher ionic strength is perhaps somewhat unexpected, but the results of the modeling of the solubility data appear unequivocal. Additional solubility experiments over a wider range of ionic strengths and temperatures are required to more fully resolve the relative importance of $Nd(OH)^{2+}$ and $Nd(OH)_2^+$.

Figure 6 shows that the solubility minimum, where $Nd(OH)_3^0$ is the predominant species, decreases with increasing temperature from 30° to at least 100 °C, but apparently increases again at 290 °C. This trend is also reflected in the temperature dependence of log Q_{s3} values given in Table 7.

Stoichiometric molal equilibrium quotients for the various hydrolysis reactions, calculated according to equation (17), are given in Tables 8, 9 and 10. The smoothed values of Q_{s0} obtained from equation (21) and given in Table 6, and the values of Q_{sn} given in Table 7 were used to derive the values of $Q_{hn,1}$. The

Table 8. Comparison of predicted and measured first hydrolysis constants of Nd^{3+}.

T(°C)	log $Q_{h1,1}$	log $K_{h1,1}$ (this study)	log $K_{h1,1}$ (Haas et al., 1995)
	I = 0.03 mol kg^{-1}		
250	-4.3±0.2	-3.8±0.3	-2.02
290	-3.9±0.2	-3.3±0.3	-1.42

NOTE: the constants tabulated refer to the equation:
$Nd^{3+} + H_2O(l) \leftrightarrow Nd(OH)^{2+} + H^+$
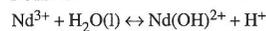
Table 9. Comparison of predicted and measured second hydrolysis constants of Nd^{3+}.

T(°C)	log $Q_{h1,1}$	log $K_{h1,1}$ (this study)	log $K_{h1,1}$ (Haas et al., 1995)
	I = 0.1 mol kg^{-1}		
290	-9.2±0.3	-8.4±0.4	-5.41

NOTE: the constants tabulated refer to the equation:
$Nd^{3+} + 2H_2O(l) \leftrightarrow Nd(OH)_2^+ + 2H^+$
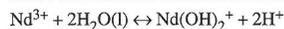
Table 10. Comparison of predicted and measured third hydrolysis constants of Nd^{3+}.

T(°C)	log $Q_{h3,1}$	log $K_{h3,1}$ (this study)	log $K_{h3,1}$ (Haas et al., 1995)
	I = 0.03 mol kg^{-1}		
30	-24.5±0.3	-24.0±0.4	-25.71
50	-24.8±0.5	-24.3±0.6	-23.33
100	-22.6±0.3	-22.1±0.4	-18.82
290	-14.9±0.3	-13.9±0.4	-10.51

NOTE: the constants tabulated refer to the equation:
$Nd^{3+} + 3H_2O(l) \leftrightarrow Nd(OH)_3^0 + 3H^+$
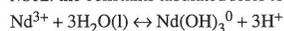
latter equilibrium quotients were extrapolated to infinite dilution using the Debye-Hückel equation (eq. 20). In addition, the reaction:

$$Nd^{3+} + 3H_2O \leftrightarrow Nd(OH)_3{}^0 + 3H^+ \qquad (23)$$

has the same ionic species, number of water molecules and charge change as does the reverse of equation (1). If it is assumed that the activity coefficient of the neutral species $Nd(OH)_3{}^0$ does not change much from 0 to 0.03 mol kg^{-1} ionic strength, then the value of $K_{h3,1}$ also can be obtained from the expression:

$$\log K_{h3,1} - \log Q_{h3,1} = \log Q_{s0} - \log K_{s0}$$
$$= I(91.51/T - 7.182 \cdot 10^{-6}T^2) - 6f^{\gamma}/\ln(10) - 3\log a_w \quad (24)$$

The values of $\log K_{h3,1}$ obtained using equation (24) differed from those obtained using the Debye-Hückel equation (eq. 20) by 0.1 log units or less. An additional ±0.1 log unit has been added to the total uncertainties in the values of $\log K_{hn,1}$ reported in Tables 8-10 to reflect the additional uncertainty inherent in extrapolation to infinite dilution.

4. DISCUSSION

4.1. Discrepancy Between Model Fit and Experimental Q_{s0} Value at 30 °C

As noted in section 3.2, equation (21) provides an excellent fit to almost all the raw Q_{s0} values given in Table 5 (Fig. 5). However, equation (21) underestimates our experimentally determined value of Q_{s0} at 30 °C and 0.03 mol kg^{-1} ionic strength by 0.64 log unit. This discrepancy may be related to a number of factors, including the lower stability of glass electrodes compared to hydrogen electrodes and less efficient stirring in the case of the 30 °C experiments (the Teflon stir bar frequently became hindered in the bottle causing stirring to stop). However, the most likely explanation is that most of the data obtained at 30 °C relate to amorphous, or at least less well-crystalline $Nd(OH)_3(s)$. Note that, the first solubility data points at 30 °C were obtained by approach from undersaturation with respect to $Nd(OH)_3(cr)$, and these lie well below the line defined by our experimentally determined value of $\log Q_{s0} = 18.6$. All other data points were obtained after NaOH had been added to raise pH_m, thus supersaturating the solution, and most of these data points lie above the line in Figure 3. Therefore, we suggest that, in the 30 °C experiments, our initial solubility measurements may relate to less soluble $Nd(OH)_3(cr)$, but after supersaturation upon addition of base, a less crystalline, more soluble form of the solid precipitated and exerted control on the measured Nd concentration. Because of the lower temperature and the less efficient stirring in the 30 °C

experiments, the solubility equilibrium was not reversible as it was in the higher temperature experiments in the HECC. In this regard it is interesting to note that the first four data points in Appendix I yield $\log Q_{s0} = 18.4 \pm 0.1$, whereas the remainder, obtained after the first addition of base, yield $\log Q_{s0} = 19.0 \pm 0.2$. The first value is in much better agreement with $\log Q_{s0} = 17.96 \pm 0.25$ obtained from equation (21). The solubility results obtained at higher temperatures are considered more reliable because reaction kinetics were more favorable, owing to the higher temperature and more efficient stirring, and hydrogen electrodes are intrinsically more stable than glass electrodes. Moreover, as shown in Figure 2 and discussed above, we were able to reverse the solubility equilibrium at the higher temperatures. Finally, because the relationship between $\log Q_{s0}$ and $1/T(K)$ is highly linear (Fig. 4), and calculation of $\log Q_{s0}$ at 30 °C from equation (21) involves an extrapolation of only 20 °C, we believe that this value of $\log Q_{s0}$ is more reliable than that obtained directly from the 30 °C experiments.

4.2. Comparison to Previous Work: Solubility Product

The value we obtain for $\log K_{s0}$ for $Nd(OH)_3$ at 25 °C and infinite dilution, via use of equation (21), is 17.9±0.3, which is more than a log unit greater than the values derived from the work of Spivakovskii and Moisa (1972, 1977), Silva (1982), Makino et al. (1993) and Rao et al. (1996), and is more than a log unit less than the value derived from the work of Morss et al. (1989). However, our value agrees to within ±0.5 log units with the estimates derived from the work of Akselrud (1963), Merli et al. (1997), and Diakonov et al. (1998), and is only 0.7 log units less than the estimate obtained by Baes and Mesmer (1986) based on the following equation relating $\log K_{s0}$ and the lattice parameter a:

$$\log K_{s0} = -103.7 + 19.04a \qquad (25)$$

The value recommended by Diakonov et al. (1998) is based on a critical evaluation of all the solubility and other thermodynamic data available at the time, and is in very good agreement with ours, being only 0.3 log units lower, which is within our experimental uncertainty. This agreement, and the extreme care we have taken in synthesizing $Nd(OH)_3(cr)$, establishing the attainment of equilibrium and measuring pH_m, lead us to believe that our value at standard conditions is the most reliable experimentally measured value available. It seems likely that, reported values of $\log K_{s0}$ that are significantly lower than ours, e.g., those of Spivakovskii and Moisa (1972, 1977), Silva

(1982), Makino et al. (1993) and Rao et al. (1996), are a result of the solubility being controlled by the formation of a surface layer of less soluble $NdOHCO_3(s)$ or $Nd_2(CO_3)_3$. As pointed out by Diakonov et al. (1998), standard X-ray diffraction may not detect such a surface precipitate, and IR spectroscopy or another more sensitive technique is required to insure its absence. Ours is the only study to have used IR spectroscopy and TGA, in addition to X-ray diffraction, to characterize the solid starting material. Diakonov et al. (1998) suggest that the NaOH solution used by Rao et al. (1996) to synthesize $Nd(OH)_3(cr)$ may have been contaminated, leading to the inadvertent formation of Nd-hydroxycarbonate or –carbonate. On the other hand, Diakonov et al. (1998) thought it unlikely that the study of Silva (1982) was affected by the same problem because Silva (1982) employed an ultrapure NaOH solution. However, we suggest that synthesis of $Nd(OH)_3(cr)$ by reacting aqueous solutions of Nd^{3+} and NaOH, is particularly susceptible to the formation of less soluble carbonate phases because of the difficulty in completely excluding CO_2 from NaOH solutions.

The only previously reported value of log K_{s0} for crystalline $Nd(OH)_3$ that is significantly greater than ours, is the value given by Morss et al. (1989). This value was calculated from calorimetric data for $Nd(OH)_3(cr)$ and literature thermodynamic data for $H_2O(l)$ and Nd^{3+}. It is well known that comparatively small relative errors in calorimetrically-derived Gibbs free energies of formation can result in much larger relative errors in the resulting Gibbs free energy of reaction, and hence the log K value, for a given chemical reaction. Such errors may be the cause of the discrepancy between our measured log K_{s0} value and the calculated value of Morss et al. (1989). On the other hand, the log K_{s0} value calculated by Merli et al. (1997) from independent, calorimetically-derived thermodynamic data for $Nd(OH)_3(cr)$ is in much closer agreement with our value.

As mentioned in the Introduction, there have been no studies of the solubility of $Nd(OH)_3$ at temperatures greater than 90 °C. Rao et al. (1996) determined K_{s0} at 25° and 90 °C for what they reported to be crystalline $Nd(OH)_3$. Their value of log K_{s0} at 25 °C (14.96) is three orders of magnitude smaller than ours (17.9), but their value at 90 °C (14.18) is more than a half an order of magnitude greater than ours (13.5). Thus, although Rao et al. (1996) observed a decrease in solubility with increased temperature, the magnitude of this decrease is considerably less than that observed in this study. Meloche and Vrátný (1959) also
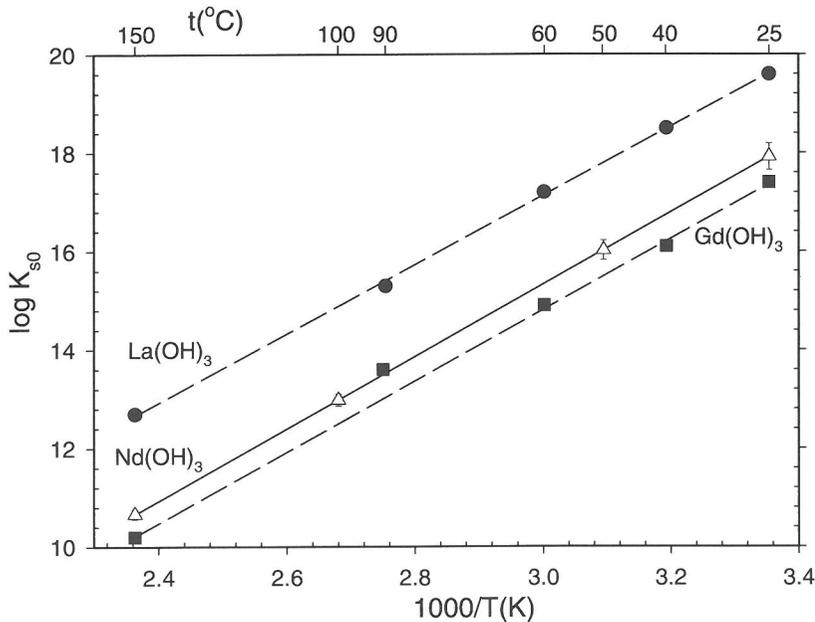
Figure 9. Plot of log K_{s0} vs. 1/T(K) for $La(OH)_3(cr)$, $Nd(OH)_3(cr)$ and $Gd(OH)_3(cr)$. The open triangles and solid line are the data and a regression line, respectively, obtained in this study. The solid symbols are the experimental data reported by Deberdt et al. (1998) and the dashed lines are regression fits to their data. For Gd, the datum at 90 °C appears to be an outlier and was omitted from the regression.

observed a decrease in the solubility of freshly pre-cipitated $Nd(OH)_3$ from 10° to 40 °C, but their values are not directly comparable to ours because their solid was likely to have been poorly crystalline.

The only reported investigation of the solubility of REE-hydroxides at temperatures above 90 °C is that of Deberdt et al. (1998), which were conducted on well-crystallized $La(OH)_3$ and $Gd(OH)_3$ up to 150 °C. The values of K_{s0} obtained by Deberdt et al. (1998) for these hydroxides are compared to the values obtained by us for $Nd(OH)_3$ in this study in Figure 9. If Deberdt et al.'s value of K_{s0} for $Gd(OH)_3$ at 90 °C, which appears to be an outlier, is neglected, then the trends for K_{s0} for all three REE hydroxides as a function of temperature are parallel. Moreover, the solubilities follow a regular pattern, i.e., La >> Nd > Gd. Thus, the two studies appear to be in very good agreement. This agreement is particularly impressive when one considers that pH was determined by quite different means in the two studies. In the study of Deberdt et al. (1998), pH was measured using glass electrodes at temperatures up to and including 90 °C, but was calculated at 150 °C.

4.3. Comparison to Previous Work: Enthalpies of Formation

From equation (21), a value of ΔH_r^o = -140.3±5.2 kJ mol^{-1} was derived for reaction (1) at infinite dilution and 25 °C (Table 6). Using values of $\Delta H_f^o(Nd^{3+})$ = -696.6 kJ mol^{-1} (Morss, 1976) and $\Delta H_f^o(H_2O)$ = -285.8 kJ mol^{-1} (SUPCRT92; Johnson et al., 1992), we obtain a value of $\Delta H_f^o(Nd(OH)_3(cr))$ = -1414±5 kJ mol^{-1}. The calorimetrically-derived values of $\Delta H_f^o(Nd(OH)_3(cr))$ reported by Merli et al. (1997), Morss et al. (1989), and Merli and Fuger (1994), respectively, are -1415.6±2.3 kJ mol^{-1}, -1403.7±1.0 kJ mol^{-1} and -1404.2±3.3 kJ mol^{-1}. The value reported by Merli et al. (1997) is in much better agreement with our enthalpy value than are the values reported by Morss et al. (1989) and Merli and Fuger (1994), which is consistent with the fact that the calculated value of log K_{s0} reported by Merli et al. (1997) is in much better agreement with our value than is the value calculated by Morss et al. (1989). Note that, in their critical evaluation, Diakonov et al. (1998) chose the value of $\Delta H_f^o(Nd(OH)_3(cr))$ reported by Merli et al. (1997) as their recommended value.

It is also of interest to compare our value of $\Delta H_f^o(Nd(OH)_3(cr))$ with the corresponding values for $La(OH)_3(cr)$, $Sm(OH)_3(cr)$ and $Am(OH)_3(cr)$. Morss and Williams (1994) report a value of $\Delta H_f^o(Am(OH)_3(cr))$ = -1371.2±7.9 kJ mol^{-1}, and Cordfunke et al. (1990) determined $\Delta H_f^o(La(OH)_3(cr))$ = -1415.5±1.4 kJ mol^{-1}. Merli et al. (1997) ob-

tained values of $\Delta H_f^o(Am(OH)_3(cr))$ = -1343.6±1.8, $\Delta H_f^o(La(OH)_3(cr))$ = -1416.7±1.3, and $\Delta H_f^o(Sm(OH)_3(cr))$ = -1406.6±2.2 kJ mol^{-1}. The two values of $\Delta H_f^o(La(OH)_3(cr))$ are indistinguishable, within the limits of error, from the value of $\Delta H_f^o(Nd(OH)_3(cr))$ suggested by this study and that of Merli et al. (1997). The value of $\Delta H_f^o(Sm(OH)_3(cr))$ is also similar to that for $Nd(OH)_3(s)$ (only 10 kJ mol^{-1} less exothermic). However, $\Delta H_f^o(Am(OH)_3(cr))$ is more than 40 kJ mol^{-1} less exothermic than $\Delta H_f^o(Nd(OH)_3(cr))$. Note also that the enthalpies of formation of $Am(OH)_3$ determined by Morss and Williams (1994) and Merli et al. (1997) differ by almost 30 kJ mol^{-1}.

4.4. Comparison to Previous Work: Hydrolysis Constants

The only hydrolysis constant that we have been able to determine near room temperature is log $Q_{h3,1}$ at 30 °C and 0.03 molal NaTr. Comparison of this value with previous work is complicated by the fact that no other low-temperature measurements were carried out at the same temperature or ionic strength (Table 2). However, our value of –24.5±0.3 at 30 °C and 0.03 mol kg^{-1} NaTr is of a similar order of magnitude to those reported by Kragten and Decnop-Weever (1984) for 21.5 °C and 1 mol L^{-1} $NaClO_4$ (log $Q_{h3,1}$ = -24.3±0.2), by Silva (1982) for 25 °C and infinite dilution (log $K_{h3,1}$ = -23.9±0.2) and Baes and Mesmer (1986) for 25 °C and infinite dilution (log $K_{h3,1}$ = -26.5). Extrapolation of our 30 °C value to infinite dilution yields a value of –24.0±0.4, which is identical within error limits to the value obtained for infinite dilution at 25 °C by Silva (1982). It is interesting to note that this difference is much less than the 1.9 log unit difference in values of log K_{s0} obtained in the two studies.

We are unaware of any experimentally-determined hydrolysis constants at elevated temperatures with which to compare our measured constants. However, Haas et al. (1995) have provided HKF parameters by which these constants may be estimated. Comparisons of values of log $K_{h1,1}$, log $K_{h2,1}$ and log $K_{h3,1}$ are given in Tables 8, 9, and 10, respectively. From Table 8 it can be seen that the values of log $K_{h1,1}$ calculated from the HKF parameters of Haas et al. (1995) are higher than those derived from our experimental data by 1.8 and 1.9 log units at 250° and 290 °C, respectively. Our value for log $K_{h2,1}$ is 3 orders of magnitude smaller than that estimated by Haas et al. (1995) (Table 9). A similar comparison of log $K_{h3,1}$ values (Table 9) shows that the estimates of Haas et al. (1995) are more than an order of magnitude smaller than our value at low temperature, but as temperature increases, the estimates of Haas et al. (1995) become larger than

our values. At 290 °C, the values of Haas et al. (1995) are larger than ours by more than three orders of magnitude. These findings suggest that use of the HKF parameters of Haas et al. (1995) will result in considerable overestimation of the degree of hydrolysis of the trivalent REE at elevated temperatures.

Other attempts to predict the hydrolysis behavior of the REE at elevated temperature have also been carried out. Wood (1990b) estimated hydrolysis constants of La^{3+}, Sm^{3+}, Lu^{3+} and Y^{3+}. Although he did not provide estimates for Nd^{3+}, comparison of our experimental results for this ion with the similar Sm^{3+} suggests that Wood (1990b) also greatly overestimated the degree of hydrolysis of the REE at elevated temperatures. Kumar (1987) estimated the degree of hydrolysis of Nd^{3+} up to 500 °C. Unfortunately, Kumar (1987) only presented his estimates in graphical form (his Fig. 1), and it is not entirely clear
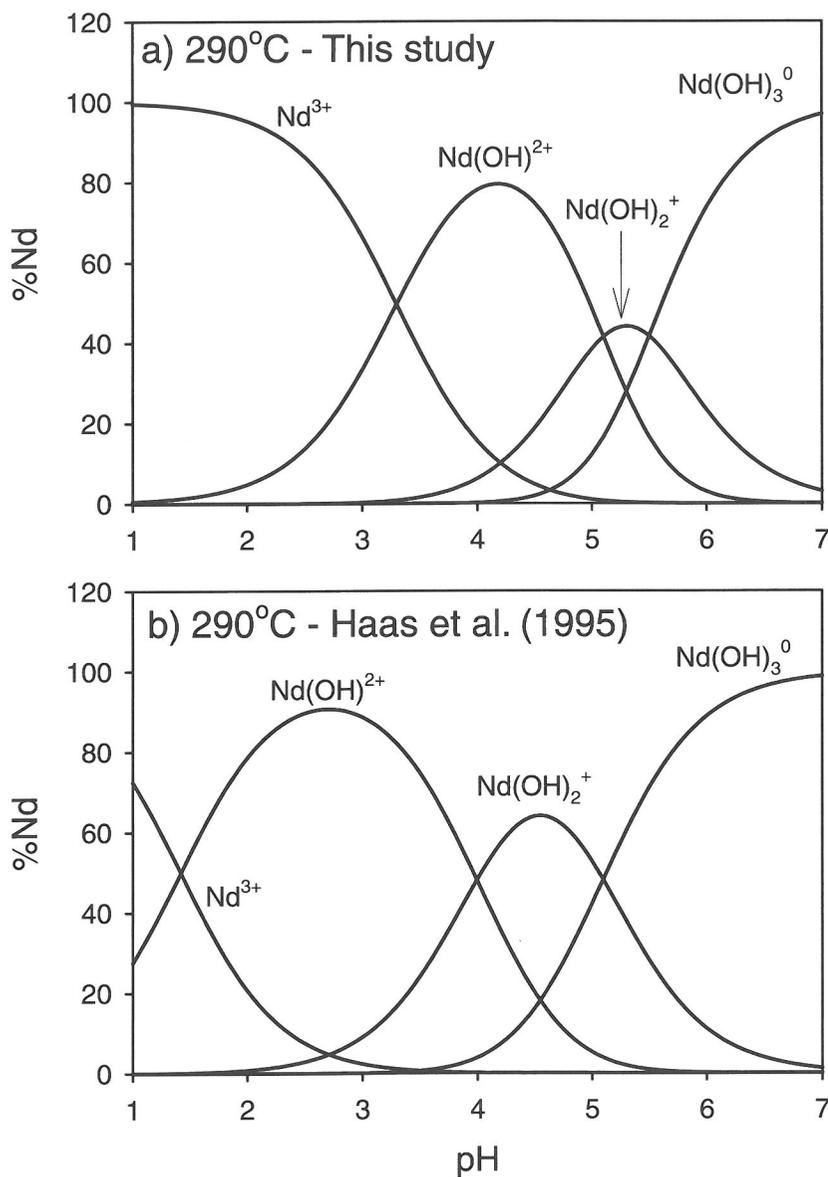

Figure 10. Plot of %Nd vs. pH at 290 °C showing the distribution of Nd^{3+} species among the various hydroxide complexes based on thermodynamic data from: a) this study; and b) Haas et al. (1995).

whether these estimates refer to infinite dilution or the ionic strength of seawater. However, his estimates of roughly $\log K_{h1,1} = -2.5$ and $\log K_{h3,1} = -12.2$ for 300 °C are much closer to our values at infinite dilution than the estimates of either Haas et al. (1995) or Wood (1990b).

Our results for the hydrolysis of Nd^{3+} are in qualitative agreement with those of Deberdt et al. (1998) for La^{3+} and Gd^{3+}. As can be seen from Figure 6, no significant hydrolysis occurs until approximately pH 8.4, 8.3 and 7.7 at 30°, 50° and 100 °C, respectively. The solubility data of Deberdt et al. (1998) reveal no evidence of hydrolysis of La^{3+} up to pH 9.5, 9.0, 8.2 and 7.0, or of Gd^{3+} up to pH 8.0, 7.4, 7.3 and 6.0 at 40°, 60°, 90° and 150 °C, respectively. The pH values noted are the highest investigated by Deberdt et al. (1998), and place upper limits on the degree of hydrolysis. In contrast, the HKF parameters of Haas et al. (1995) would predict a species change from La^{3+} to $La(OH)_3^0$ at pH 8.7, 7.9, 7.0 and 5.6 and from Gd^{3+} to $Gd(OH)_3^0$ at pH 7.8, 7.1, 6.2, and 5.0 at 40°, 60°, 90° and 150 °C, respectively. Thus, the results of Deberdt et al. (1998) confirm our conclusion that the HKF parameters of Haas et al. (1995) increasingly overestimate the degree of hydrolysis of the trivalent REE as temperature increases.

The speciation diagrams depicted in Figure 10 compare the predicted distribution at 290 °C, as a function of pH, of Nd^{3+} species that arises using the theoretical estimates of Nd^{3+} hydrolysis constants calculated from the HKF parameters of Haas et al. (1995), with that arising from the use of our experimentally-determined constants given in Tables 8-10. The Haas et al. (1995) constants predict that hydroxide complexes predominate over Nd^{3+} at a pH of less than 1.5 at this temperature, whereas our data predict that hydroxide complexes do not predominate until pH = 3. The Haas et al. (1995) constants also predict a larger predominance field for $Nd(OH)_2^+$ than do our data. Finally, in the Haas et al. (1995) speciation model, $Nd(OH)_3^0$ becomes predominant at a pH almost one unit lower than in our model. These differences will result in a substantial overestimation of the solubility of Nd-bearing solid phases in the absence of other complexation agents. Moreover, in previous work we have demonstrated that the HKF parameters of Haas et al. (1995) and Shock and Koretsky (1993) underestimate the stability constants of Nd-chloride (Gammons et al., 1996 and this volume) and Nd-acetate complexes (Wood et al., 2000; Ding and Wood, this volume). Thus, use of stability constants for Nd complexes from Haas et al. (1995) and Shock and Koretsky (1993) will result in serious overestimation of the importance of hydroxide complexes relative to chloride and/or acetate complexes in hydrothermal solutions.

Figure 11 illustrates how calculated solubility of $Nd(OH)_3(cr)$ as a function of pH depends sensitively on the precise values of $Q_{hn,1}$. In both Figures 11a and 11b, the value of Q_{s0} obtained in this study at 290 °C was used to calculate the concentration of Nd^{3+} in equilibrium with $Nd(OH)_3(cr)$ as a function of pH. In Figure 11a, the values of $K_{hn,1}$ obtained in this study were employed to calculate the concentrations of the hydroxide complexes, whereas in Figure 11b, the estimates of Haas et al. (1995) were used. It is obvious that the calculated total solubility of Nd^{3+} is much higher in Figure 11b than in Figure 11a. Thus, use of the HKF parameters of Haas et al. (1995) for hydroxide complexes of the REE in calculations of the solubility of REE minerals in the absence of other ligands is likely to result in significant overestimation of the total equilibrium REE concentration at saturation.

4.5. Polynuclear Species

A number of workers have identified polynuclear hydrolysis products of Nd^{3+}, e.g., $Nd_2(OH)_3^{4+}$ and $Nd_3(OH)_5^{4+}$ (cf. Baes and Mesmer, 1986 and references therein; Kragten and Decnop-Weever, 1984). We have detected no evidence for such products in our solubility data. According to the following reactions:

$$2Nd(OH)_3(cr) + 4H^+ \leftrightarrow Nd_2(OH)_3^{4+} + 4H_2O(l) \quad (26)$$

$$3Nd(OH)_3(cr) + 4H^+ \leftrightarrow Nd_3(OH)_5^{4+} + 4H_2O(l) \quad (27)$$

the slope of a curve of $\log \Sigma Nd$ vs. pH should yield a value of -4 if either $Nd_2(OH)_2^{4+}$ or $Nd_3(OH)_5^{4+}$ were a predominant species over any range of pH investigated. None of our data correspond to such a slope. In fact, as shown in Figure 3, the data tend to exhibit slopes slightly more shallow than -3. Thus, we conclude that polynuclear species of the type previously proposed, are present in concentrations too low to contribute significantly to our measured solubilities. This conclusion is supported by the fact that calculations carried out using the thermodynamic data given in Baes and Mesmer (1986) for the solubility of $Nd(OH)_3(cr)$ and the hydrolysis of Nd^{3+} at 25 °C also indicate that $Nd_2(OH)_2^{4+}$ is never a significant species over the pH range we investigated, when the total Nd concentration is constrained to a low level by the solubility of $Nd(OH)_3(cr)$.

We cannot rule out entirely the possibility that polynuclear species of stoichiometries different from the two mentioned above were present in significant concentrations in our experiments. However, there are a number of reasons to suspect that polynuclear species were not present in significant quantity, including: 1) we have obtained excellent fits of our

models to the solubility data without invoking any polynuclear species; 2) the stability of polynuclear species is strongly dependent on the total concentration of Nd, which is comparatively low in equilibrium with $Nd(OH)_3(s)$ in our experiments; and 3) the stability of polynuclear species tends to decrease with increasing temperature (cf. Wesolowski et al., 1984; Plyasunov and Grenthe, 1994).
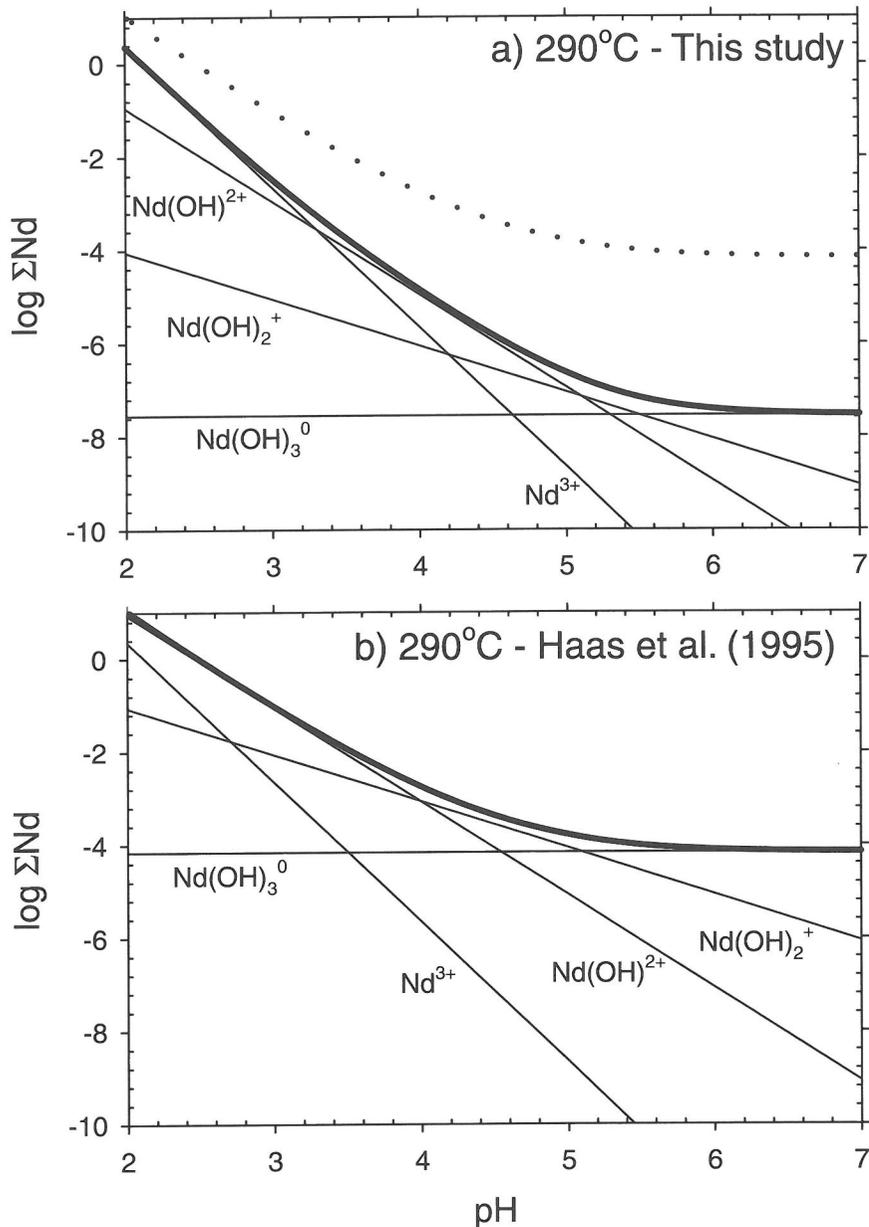
Figure 11. Calculated solubilities of $Nd(OH)_3(cr)$ at 290 °C and infinite dilution presented in the form of plots of log $m_{\Sigma Nd}$ vs. pH. Both diagrams were calculated using the value of K_{s0} obtained in this study and the values of hydrolysis constants: a) determined in this study; and b) estimated by Haas et al. (1995). The heavy line and the light lines in each diagram represent the calculated total Nd concentration in solution and the calculated concentrations of individual species, respectively. To aid comparison, the calculated total solubility from b) is reproduced in a) as the dotted line.

4.6. Comparison of Solubilities of Nd(OH)$_3$, Am(OH)$_3$ and Pu(OH)$_3$

Owing to the use of trivalent REE as analogues of the trivalent actinides, it is of interest to compare the solubility of Nd(OH)$_3$ to those of the corresponding hydroxides of some trivalent actinides. Table 11 summarizes reported values of the solubility product (log Q$_{s0}$) for Am(OH)$_3$ and Pu(OH)$_3$. In many cases, the crystallinity of the initial solid phase is not clear. However, it is evident that the reported values of log Q$_{s0}$ for the hydroxides of Am and Pu scatter over similar ranges as that given in Table 1 for Nd-hydroxide.

The only author to have measured the solubilities of both Nd(OH)$_3$ and Am(OH)$_3$ using the same conditions and techniques was Silva (1982), and his reported solubility products for these two hydroxides are identical within experimental error. Because there is some uncertainty as to the quality of the solubility data obtained by Silva (1982) for Nd, the similarity in his measured solubilities of Nd- and Am-hydroxides cannot be taken as definitive. However, it is worthwhile noting that the recommended solubility products for these two hydroxides given by Baes and Mesmer (1986), based on equation (25) are also nearly identical, owing to their nearly identical cell parameters. It is also interesting to note that the solubility product obtained by Rai et al. (1983) for Am(OH)$_3$ is very close to the value we have obtained for Nd(OH)$_3$, although values for Am(OH)$_3$ determined subsequently by other authors are not in good agreement with our value for Nd(OH)$_3$. One might actually expect that the solubility of the actinide hydroxides should be somewhat higher owing to the effects of radioactivity. However, because of the large spread in measured values of the solubility product for all three of the hydroxides in question, it would appear that the only way to definitively compare their solubilities would be to determine the solubilities of the actinide hydroxides using the same techniques employed in this paper for Nd(OH)$_3$.

5. CONCLUSIONS

We have determined the solubility of Nd(OH)$_3$(cr) as a function of pH, ionic strength (0.03-1.0 m) and temperature (30°-290 °C) in non-complexing Na-triflate media using *in-situ* pH measurements in a well-stirred, hydrogen-electrode concentration cell. The following conclusions can be drawn from this work:

1. In our well-stirred reaction cell, equilibrium is attained within 0.5-1 days at 150 °C, and within a few hours at 290 °C.
2. The un-hydrolyzed, un-complexed Nd^{3+} ion is the predominant species over the majority of the pH range investigated.
3. Log Q$_{s0}$ values obtained in this study decrease with increasing temperature, i.e., Nd(OH)$_3$(cr) exhibits retrograde solubility, and are a linear function of 1/T(K).
4. The log Q$_{s0}$ values obtained in this study are well described by the simple expression: log Q$_{s0}$ = -6.662 + 7300.0/T + I(-91.51/T − 7.182·10^{-6}T^2) − 6f$^\gamma$/ln(10) − 3log a$_w$.

Table 11. Summary of literature data on the solubility of Am(OH)$_3$(s) and Pu(OH)$_3$(s) at room temperature.

Author	T(°C)	Ionic strength and medium	log Q$_{s0}$
Am^{3+}			
Allard et al. (1978)	25	infinite dilution	14[1]
Phillips (1982)	25	infinite dilution	18.7[1]
Silva (1982)	25	0.1 mol L^{-1} NaClO$_4$ (extr. to 0 with Davies eq.)	15.9±0.4[2]
Rai et al. (1983)	25	0.003 mol L^{-1} CaCl$_2$ (extr. to 0 with Pitzer eq.)	17.5±0.3[2]
Bernkopf & Kim (1984)	25	0.1 mol L^{-1} NaClO$_4$	13.9[2]
Baes & Mesmer (1986)	25	infinite dilution	18.7[1]
Stadler & Kim (1988)	25	0.1 mol L^{-1} NaClO$_4$	16.3±0.3[2]
Morss & Williams (1994)	25	infinite dilution	15.5±2[3,5]
	25	"	12.5±1.6[3,6]
Silva et al. (1995)	25	"	15.2±0.6[4]
Merli et al. (1997)	25	"	16.8[3]
Pu^{3+}			
Busey & Cowan (1950)	25	infinite dilution	22.4
Latimer (1952)	25	infinite dilution	22.3[1]
Felmy et al. (1989)	25	infinite dilution	15.8±0.4[2]
Morss & Williams (1994)	25	infinite dilution	14.5±2[3]

NOTE: K$_{s0}$ and Q$_{s0}$ refer to the reactions: Am(OH)$_3$(s) + 3H$^+$ ↔ Am^{3+} + 3H$_2$O(l) or Pu(OH)$_3$(s) + 3H$^+$ ↔ Pu^{3+} + 3H$_2$O(l) and are given in the same units as the ionic strength.
[1]Estimated values;
[2]Directly measured experimentally;
[3]Calculated from calorimetrically-derived thermodynamic data;
[4]Based on critical evaluation of the literature;
[5]Calculated based on calorimetrically-determined value of ΔH$_f$°(Am(OH)$_3$(cr)) by Morss and Williams (1994);
[6]Recommend value of Morss and Williams (1994) based on critical evaluation.

5. Extrapolation of our results to infinite dilution and 25 °C yields a value of $\log K_{s0} = 17.9\pm0.1$, in excellent agreement with a recent critical evaluation by Diakonov et al. (1998).

6. Our solubility results for $Nd(OH)_3(cr)$ as a function of temperature are consistent with the results of Deberdt et al. (1998) for $La(OH)_3(cr)$ and $Gd(OH)_3(cr)$.

7. At low temperature (30°-150 °C), hydrolysis proceeds very rapidly over a narrow pH range from Nd^{3+} to $Nd(OH)_3^0$, with little evidence of intermediate species such as $Nd(OH)^{2+}$ or $Nd(OH)_2^+$.

8. At high temperature (250°-290 °C), the intermediate species $Nd(OH)^{2+}$ and $Nd(OH)_2^+$ become more important, but the relative importance of these two species appears to be strongly dependent on ionic strength.

9. Hydrolysis constants derived from our data at elevated temperatures are much smaller than predicted by recent theoretical estimates.

10. The value of $\Delta H_f^o(Nd(OH)_3(cr)) = -1414\pm5$ kJ mol^{-1}, derived from the temperature dependence of $\log K_{s0}$, compares well with calorimetrically-derived values.

Our results clearly demonstrate that the techniques employed in this study are capable of producing high-quality solubility data for REE hydroxides. It should be possible to use the same techniques to obtain data of comparable quality on a range of REE hydroxides, as well as hydroxides of actinide analogues. Finally, it should be possible to use the study reported here as a foundation from which the complexation of Nd^{3+} with a variety of ligands, such as chloride, sulfate, acetate, EDTA, etc. can be investigated at elevated temperatures. Some preliminary experiments with acetate in our laboratories have indeed shown promise in this regard.

Editorial handling: T.H. Giordano

REFERENCES

Akselrud N. V. (1963) Basic chlorides and hydroxides of elements of the scandium and lanthanoid group. *Usp. Khim.* **32**, 800-822 (in Russian).

Allard B., Kipatsi H. and Torstenfelt B. (1978) Sorption an Langlivade Radionuklider. Karnbranslesakerhet, Stockholm, Lera Och Berg Del 2, KBS-98.

Azhipa L. T., Kovalenko P. N., and Evstifeev M. M. (1967) Oscillographic determination of the pH of precipitation and activity products of ytterbium and neodymium hydroxides. *Russ. Jour. Inorg. Chem.* **12**, 601-603.

Baes C. F. Jr. and Mesmer R. E. (1986) The Hydrolysis of Cations (Reprint with corrections of the 1976 edition by John Wiley & Sons), Robert E. Krieger. Malabar, Florida.

Bénézeth P., Palmer D. A., and Wesolowski D. J. (1997) The aqueous chemistry of aluminum. A new approach to high temperature solubility measurements. *Geothermics* **26**, 465-481.

Bénézeth P., Palmer D. A., and Wesolowski D. J. (1999) The solubility of zinc oxide in 0.03 m NaTr as a function of temperature, with in situ pH measurement. *Geochim. Cosmochim. Acta* **63**, 1571-1586.

Bénézeth P., Palmer D. A., and Wesolowski D. J. (2001) Aqueous high-temperature solubility studies: II. The solubility of boehmite at 0.03 m ionic strength as a function of temperature and pH as determined by "in situ" measurements. *Geochim. Cosmochim. Acta* **65**, 2097-2111.

Bernkopf M. and Kim J. I. (1984) Hydrolysis reactions and carbonate complexation of americium(III) in natural aquatic systems. Report RCM-02884.

Brush L. H. (1990) Test plan for laboratory and modeling studies of repository and radionuclide for the waste isolation pilot program. Sandia Report.

Burkov K. A., Lilich L. S., Ngo N. D., and Smirnov A. Yu. (1973) Potentiometric study of the hydrolysis of neodymium ions (Nd^{3+}) in 3 M (Na)ClO$_4$ solution. *Russ. Jour. Inorg. Chem.* **18**, 797-800.

Burkov K. A., Busko E. A., and Lilich L. C. (1988) On the hydrolysis of rare earth element metal ions. *Zh. Neorg. Khim.* **33**, 339-342.

Busey H. M. and Cowan H. D. (1950) Behavior of plutonium(III) chloride in titrations with acid and base. LAMS-1105, Los Alamos National Laboratory, Los Alamos, NM.

Busing W. R., Levy H. A. (1962) A General Fortran Least Squares Program, Oak Ridge Natl. Lab. Rep. ORNL-TM-271.

Caro P. E., Sawyer J. O., and Eyring L. (1972) The infrared spectra of rare earth carbonates. *Spectrochim. Acta* **28A**, 1167-1173.

Choppin G. R. (1983) Comparison of the solution chemistry of the actinides and lanthanides. *Jour. Less-Common Metals* **93**, 323-330.

Choppin G. R. (1986) Speciation of the trivalent *f*-elements in natural waters. *J. Less-Common Met.* **126,** 307-313.

Choppin G. R. (1989) Soluble rare earth and actinide species in seawater. *Mar. Chem.* **28**, 19-26.

Christensen A. N. (1966) Hydrothermal preparation of some rare earth trihydroxides and rare earth oxide hydroxides. *Acta Chem. Scand.* **20**, 896-899.

Cordfunke E. H. P., Konings R. J. M., and Ouweltjes W. (1990) The standard enthalpies of formation of hydroxides. IV. La(OH)$_3$ and LaOOH. *Jour. Chem. Thermo.* **22**, 449-452.

Deberdt S., Castet S., Dandurand J.-L., Harrichoury J.-C., and Louiset, I. (1998) Experimental study of La(OH)$_3$

and Gd(OH)$_3$ solubilities (25 to 150 °C), and La-acetate complexing (25 to 80 °C). *Chem. Geol.* **151**, 349-372.

Diakonov I. I., Tagirov B. R., and Ragnarsdottir K. V. (1998) Standard thermodynamic properties and heat capacity equations for rare earth element hydroxides. I. La(OH)$_3$ and Nd(OH)$_3$. Comparison of thermochemical and solubility data. *Radiochim. Acta* **81**, 107-116.

Dickson A. G., Wesolowski D. J., Palmer D. A., and Mesmer R. E. (1990) Dissociation constant of bisulfate ion in aqueous sodium chloride solutions to 250 °C. *Jour. Phys. Chem.* **94**, 7978-7985.

Ding R. and Wood S. A. (this volume) The aqueous geochemistry of the rare earth elements and yttrium. Part X. Potentiometric determination of stability constants of acetate complexes of La^{3+}, Nd^{3+}, Gd^{3+} and Yb^{3+} at 25-70 °C and 1 bar.

Felmy A. R., Rai D., Schramke J. A., and Ryan J. L. (1989) The solubility of plutonium hydroxide in dilute solution and in high-ionic-strength chloride brines. *Radiochim. Acta* **48**, 29-35.

Gammons C. H., Wood S. A., and Williams-Jones A. E. (1996) The aqueous geochemistry of the rare earth elements and yttrium: VI. Stability of neodymium chloride complexes at 25 °C to 300 °C. *Geochim. Cosmochim. Acta* **60**, 4615-4630.

Guillaumont R., Désiré B., and Galin M. (1971) Première constante d'hydrolyse des lanthanides. *Radiochem. Radioanal. Let.* **8**, 189-198.

Haas J. R., Shock E. L., and Sassani D. C. (1995) Rare earth elements in hydrothermal systems: Estimates of standard partial molal thermodynamic properties of aqueous complexes or the rare earth elements at high pressures and temperatures. *Geochim. Cosmochim. Acta* **59**, 4329-4350.

Helgeson H. C. and Kirkham D. H. (1974) Theoretical prediction of the thermodynamic properties of aqueous electrolytes at high pressures and temperatures: II. Debye-Hückel parameters for activity. *American Journal of Science* **274**, 1199-1261.

Ho P.C. and Palmer D. A. (1995) Electrical conductivity measurements of dilute aqueous sodium trifluoromethanesulfonate solutions at temperatures 0-450 °C and pressures up to 250 MPa. *Jour. Sol. Chem.* **24**, 753-769.

Johnson J. W., Oelkers E. H., and Helgeson H. C. (1992) SUPCRT92: a software package for calculating the standard molal thermodynamic properties of minerals, gases, aqueous species, and reactions from 1-5000 bars and 0-1000 °C. *Comp. Geosci.* **18**, 899-947.

Klevtsov P. V., Klevtsova R. F., and Sheina L. P. (1967) Relationship between the infrared absorption spectra and crystal structure of the hydroxides of the rare earth elements and yttrium. *Jour. Struct. Chem.* **8**, 229-233.

Kostromina N. A., and Badaev Yu. B. (1986) Spectrophotometric study of hydrolysis in the NdCl$_3$-KOH system. *Ukrain. Khim. Zhur.* **52**, 793-796.

Kragten J. and Decnop-Weever L. G. (1984) Hydroxide complexes of lanthanides - VII. Neodymium(III) in perchlorate medium. *Talanta* **31**, 731-733.

Kumar M. D. (1987) Cation hydrolysis and the regulation of trace metal composition in seawater. *Geochim. Cosmochim. Acta* **51**, 2137-2145.

Latimer W. M. (1952) Oxidation Potentials, 2nd ed., Prentice-Hall, New York.

Liu C. and Lindsay W.T. Jr. (1972) Thermodynamics of sodium chloride solutions at high temperatures. *Jour. Sol. Chem.* **1**, 45-69.

Makino H., Yajima T., Yoshikawa H., Yui M. and Sasaki N. (1993) Neodymium(III) hydrolysis constants and solubil-

ities of Nd(III) hydroxide. *Nippon Kagaku Kaishi* **5**, 445-450 (in Japanese; Chem. Abstr. 119: 81217b).

Meloche C. C. and Vrátný F. (1959) Solubility product relations in the rare earth hydrous hydroxides. *Anal. Chim. Acta* **20**, 415-418.

Merli L. and Fuger J. (1994) Thermochemistry of a few neptunium and neodymium oxides and hydroxides. *Radiochim. Acta* **66/67**, 109-113.

Merli L., Lambert B., and Fuger J. (1997) Thermochemistry of lanthanum, neodymium, samarium and americium trihydroxides and their relation to the corresponding hydroxycarbonates. *Jour. Nucl. Mater.* **247**, 172-176.

Mesmer R. E. (1991) Comments on "A new approach to measuring pH in brines and other concentrated electrolytes" by K.G. Knauss, T.J. Wolery, and K.J. Jackson. *Geochim. Cosmochim. Acta* **55**, 1175-1176.

Millero F. J. (1992) Stability constants for the formation of rare earth inorganic complexes as a function of ionic strength. *Geochim. Cosmochim. Acta* **56**, 3123-3132.

Moeller T. (1946) Observations on the rare earths. LV. Hydrolysis studies upon yttrium and certain rare earth(III) sulfate solutions at 25 °C. *Jour. Phys. Chem.* **50**, 242-250.

Moeller T. and Fogel N. (1951) Observations on the rare earths. LXI. Precipitation of hydrous oxides or hydroxides from perchlorate solutions. *Jour. Amer. Chem. Soc.* **73**, 4481.

Moeller T. and Kremers H. E. (1944) Observations on the rare earths. LI. An electrometric study of the precipitation of trivalent hydrous rare earth oxides or hydroxides. *Jour. Phys. Chem.* **48**, 395-406.

Moeller T., Martin D. F., Thompson L. C., Ferrus R., Feistel R., and Randall W.J. (1965) The coordination chemistry of yttrium and the rare earth metal ions. *Chem. Rev.* **65**, 1-50.

Morss L. R. (1976) Thermochemical properties of yttrium, lanthanum, and the lanthanide elements and ions. *Chem. Rev.* **76**, 827-841.

Morss L. R. and Williams C. W. (1994) Synthesis of crystalline americium hydroxide, Am(OH)$_3$, and determination of the solubility-product constants of actinide(III) hydroxides. *Radiochim. Acta* **66/67**, 89-93.

Morss L. R., Haar C. M., and Mroczkowski S. (1989) Standard molar enthalpy of formation of neodymium hydroxide. *Jour. Chem. Thermo.* **21**, 1079-1083.

Mroczkowski S., Eckert J., Meissner H., and Doran J. C. (1970) Hydrothermal growth of single crystals of rare earth hydroxides. *Jour. Cryst. Growth* **7**, 333-342.

Nitsche H. (1990) Basic research for assessment of geologic nuclear waste repositories: What solubility and speciation studies of transuranium elements can tell us. Paper presented at the Intl. Symp. on Sci. Basis for Nuclear Waste Management, Boston, MA Conf. Proceedings.

Orhanovic Z., Pokric B., Füredi H., and Branica M. (1966) Precipitation and hydrolysis of metallic ions. III. Studies on the solubility of yttrium and some rare earth hydroxides. *Croat. Chem. Acta* **38**, 269-276.

Palmer D. A. and Hyde K. E. (1993) Ferrous chloride and acetate complexation in aqueous solutions at high temperatures. *Geochim. Cosmochim. Acta* **57**, 1393-1408.

Palmer D. A. and Wesolowski D. J. (1993) Aluminum speciation and equilibria in aqueous solution: Potentiometric determination of the first hydrolysis constant of aluminum(III) in sodium chloride solutions to 125 °C. *Geochim. Cosmochim. Acta* **57**, 2929-2938.

Palmer D. A., Bénézeth P., and Wesolowski D. J. (2001) Aqueous high-temperature solubility studies. I. The solubility of boehmite as functions of ionic strength (to 5 molal NaCl), temperature (100-250 °C) and pH as deter-

mined by in situ measurements. *Geochim. Cosmochim. Acta* **65**, 2081-2095.

Phillips S. L. (1982) Hydrolysis and formation constants at 25 °C. U.S. DOE Report LBL-14313.

Pitzer K. S., Roy R. N., and Silvester L. F. (1977) Thermodynamics of electrolytes. 7. Sulfuric acid. *Jour. Amer. Chem. Soc.* **99**, 4930-4936.

Plyasunov A. V. and Grenthe I. (1994) The temperature dependence of stability constants for formation of polynuclear cationic complexes. *Geochim. Cosmochim. Acta* **58**, 3561-3582.

Quist A. S. and Marshall W. L. (1965) Assignment of limiting equivalent conductances for single ions to 400°C. *Jour. Phys. Chem.* **69**, 2984-2987.

Rai D., Strickert R. G., Moore D. A., and Ryan J. L. (1983) Am(III) hydrolysis constants and solubility of Am(III) hydroxide. *Radiochim. Acta* **33**, 201-206.

Rao L., Rai D., and Felmy A. R. (1996) Solubility of Nd(OH)$_3$(c) in 0.1 M NaCl aqueous solution at 25°C and 90 °C. *Radiochim. Acta* **72**, 151-155.

Robinson R. A. and Stokes R. H. (1959) Electrolyte Solutions. Butterworths. London, UK.

Roy R. and McKinstry H. A. (1953) So-called Y(OH)$_3$-type structure, and structure of La(OH)$_3$. *Acta Cryst.* **6**, 365-366.

Shafer M. W. and Roy R. (1959) Rare-earth polymorphism and phase equilibria in rare-earth oxide-water systems. *Jour. Amer. Ceram. Soc.* **42**, 563-570.

Shock E. L. and Koretsky C. M. (1993) Metal-organic complexes in geochemical processes: Calculation of standard partial molal thermodynamic properties of aqueous acetate complexes at high pressures and temperatures. *Geochim. Cosmochim. Acta* **57**, 4899-4922.

Silva R. J. (1982) The solubilities of crystalline neodymium and americium trihydroxides. Berkeley, California, Lawrence Berkeley Laboratory, University of California. Thermodynamic Properties of Chemical Species in Nuclear Waste. Topical Report, 57 p.

Silva R. J., Bidoglio G., Rand M. H., Robouch P. B., Wanner H., and Puigdomenech I. (1995) Chemical Thermodynamics of Americium. NEA-OECD Publication, Paris/North-Holland Elsevier, Amsterdam.

Spivakovskii V. B. and Moisa L. P. (1972) Conditions of precipitation of neodymium hydroxide and hydroxide chlorides. *Russ. Jour. Inorg. Chem.* **17**, 34-37.

Spivakovskii V. B. and Moisa L. P. (1977) Composition, activity products, and free energies of formation of scandium, yttrium, lanthanum, and lanthanide hydroxide chlorides and hydroxides. *Russ. Jour. Inorg. Chem.* **22**, 643-646.

Stadler S. and Kim J. I. (1988) Hydrolysis reactions of Am(III) and Am(V). *Radiochim. Acta* **44/45**, 39-44.

Tobias R. S. and Garrett A. B. (1958) The thermodynamic properties of neodymium hydroxide Nd(OH)$_3$, in acid, neutral and alkaline solutions at 25°; the hydrolysis of the neodymium and praseodymium ions, Nd^{3+}, Pr^{3+}. *Jour. Amer. Chem. Soc.* **80**, 3532-3537.

Viswanathiah M. N., Tareen J. A. K., and Kutty T. R. (1976) Hydrothermal equilibria in Ln$_2$O$_3$-H$_2$O systems for neodymium, samarium, ytterbium and yttrium. *Ind. Mineral.* **17**, 54-59.

Viswanathiah M. N., Tareen J. A. K., and Kutty T. R. (1980) Hydrothermal phase equilibria studies in Ln$_2$O$_3$-H$_2$O systems and synthesis of cubic lanthanide oxides. *Mat. Res. Bull.* **15**, 855-859.

Wesolowski D. J. and Palmer D. A. (1994) Aluminum speciation and equilibria in aqueous solution: V. Gibbsite solubility at 50 °C and pH 3-9 in 0.1 molal NaCl solutions (a general model for aluminum speciation; analytical methods). *Geochim. Cosmochim. Acta* **58**, 2947-2969.

Wesolowski D. J., Bénézeth P., and Palmer D. A. (1998) ZnO solubility and Zn^{2+} complexation by chloride and sulfate in acidic solutions to 290 °C with in-situ pH measurement. *Geochim. Cosmochim. Acta* **62**, 971-984.

Wesolowski D. J., Drummond S. E., Mesmer R. E., and Ohmoto H. (1984) Hydrolysis equilibria of tungsten(VI) in aqueous sodium chloride solutions to 300 °C. *Inorg. Chem.* **23**, 1120-1132.

Wood S. A. (1990a) The aqueous geochemistry of the rare-earth elements and yttrium. 1. Review of available low-temperature data for inorganic complexes and the inorganic REE speciation of natural waters. *Chem. Geol.* **82**, 159-186.

Wood S. A. (1990b) The aqueous geochemistry of the rare-earth elements and yttrium. 2. Theoretical prediction of speciation in hydrothermal solutions to 350 °C at saturation water vapor pressure. *Chem. Geol.* **88**, 99-125.

Wood S. A., Wesolowski D. J., and Palmer D. A. (2000) The aqueous geochemistry of the rare earth elements: IX. A potentiometric study of Nd^{3+} complexation with acetate in 0.1 molal NaCl solution from 25-250 °C. *Chem. Geol.* **167**, 231-253.

APPENDIX

APPENDIX I. Raw data for Nd(OH)$_3$(cr) solubility experiments at 30.1±0.1°C and 1 bar in 0.03 molal Na-triflate.

Sample No.	Time (days)	pH	log m_{Nd}
Nd-1-30-1	2	7.01	-2.73
Nd-1-30-2	6	7.06	-2.77
Nd-1-30-3	7	7.12	-2.78
Nd-1-30-4	8	7.08	-2.77
Nd-1-30-5	9	7.39	-3.21
Nd-1-30-6	10	7.46	-3.28
Nd-1-30-11	28	8.39	-6.32
Nd-1-30-12	30	8.31	-6.29
Nd-1-30-13	35	8.06	-5.44
Nd-1-30-14	38	7.76	-4.18
Nd-1-30-15	40	7.71	-4.02
Nd-1-30-16	42	7.25	-2.76
Nd-1-30-17	45	7.26	-2.74
Nd-1-30-24	73	9.13	-6.61
Nd-1-30-25	78	9.09	-6.38

APPENDIX II. Raw data for $Nd(OH)_3(cr)$ solubility
experiments at elevated temperatures in Na-triflate medium.

Sample No.	Time (hours)	T(°C)	P(bars)	I (mol kg^{-1})	pH	log m$_{\Sigma Nd}$
Nd-1-150-1	68	150.1	21.5	0.0298	5.473	-5.01
Nd-1-150-2	92	150.1	21.1	0.0298	5.447	-5.05
Nd-1-150-3	116	150.1	22.2	0.0301	5.198	-4.15
Nd-1-150-4	140	150.1	21.7	0.0301	5.200	-4.17
Nd-1-150-5	164	150.1	22.1	0.0298	5.360	-4.63
Nd-1-150-6	172	150.1	22.6	0.0298	5.359	-4.62
Nd-1-150-7	191	150.1	23.1	0.0298	5.359	-4.62
Nd-1-150-11	244	150.1	25.2	0.0297	5.770	-5.98
Nd-1-150-12	259	150.1	24.1	0.0297	5.552	-5.23
Nd-1-150-13	268	150.1	23.2	0.0297	5.552	-5.19
Nd-1-200-1	284	200.1	34.7	0.0298	5.084	-5.46
Nd-1-200-2	292	200.1	35.8	0.0298	5.088	-5.32
Nd-1-200-3	308	200.1	40.3	0.0299	4.772	-4.59
Nd-1-200-4	317	200.1	43.5	0.0300	4.780	-4.55
Nd-1-200-5	332	200.1	52.1	0.0304	4.546	-3.94
Nd-1-200-6	340	200.1	52.0	0.0304	4.541	-3.94
Nd-1-200-7	363	200.1	68.5	0.0307	4.475	-3.75
Nd-1-200-8	385	200.1	71.7	0.0310	4.419	-3.62
Nd-1-200-9	404	200.1	74.0	0.0299	4.724	-4.43
Nd-1-250-1	428	250.1	105.1	0.0301	4.365	-4.58
Nd-1-250-2	436	250.1	106.6	0.0301	4.373	-4.62
Nd-1-250-3	452	250.1	110.2	0.0300	4.713	-5.30
Nd-1-250-4	460	250.1	124.4	0.0300	4.733	-5.40
Nd-1-250-5	476	250.1	124.3	0.0300	4.861	-5.64
Nd-1-250-6	484	250.2	124.4	0.0300	4.873	-5.85
Nd-1-250-7	501	250.1	124.5	0.0301	4.778	-5.58
Nd-1-250-8	506	250.1	124.1	0.0302	4.787	-5.62
Nd-1-250-9	529	250.1	129.6	0.0303	4.546	-5.09
Nd-1-250-10	548	250.1	130.2	0.0304	4.352	-4.62
Nd-1-250-11	573	250.1	135.5	0.0306	4.168	-4.15
Nd-1-250-12	580	250.1	138.1	0.0310	4.026	-3.78
Nd-1-250-13	596	250.1	144.4	0.0322	3.873	-3.37
Nd-2-50-1	28	50.1	10.5	0.0308	6.685	-3.59
Nd-2-50-2	52	50.1	10.1	0.0308	6.686	-3.59
Nd-2-50-3	72	50.1	9.6	0.0308	6.684	-3.59
Nd-2-50-4	92	50.1	10.4	0.0315	6.581	-3.34
Nd-2-50-5	100	50.1	10.3	0.0325	6.498	-3.13
Nd-2-50-6	116	50.2	10.1	0.0318	6.573	-3.22
Nd-2-50-7	164	50.2	9.6	0.0306	6.671	-3.43
Nd-2-50-10	196	50.2	8.7	0.0286	7.376	-5.52
Nd-2-50-11	215	50.2	12.8	0.0285	7.546	-6.34
Nd-2-50-12	239	50.2	11.3	0.0286	6.995	-4.46
Nd-2-50-13	260	50.1	11.3	0.0286	6.997	-4.46
Nd-2-50-14	268	50.2	11.1	0.0284	7.285	-5.28
Nd-2-50-15	284	50.1	10.5	I 0.0284	7.269	-5.26
Nd-2-50-16	292	50.2	10.2	0.0284	7.264	-5.23
Nd-2-50-17	308	50.1	10.0	0.0284	7.466	-5.87
Nd-2-50-18	313	50.2	10.9	0.0284	7.457	-5.91
Nd-2-50-19	339	50.2	10.5	0.0284	8.888	-7.91
Nd-2-50-20	363	50.2	10.1	0.0284	8.856	-8.75
Nd-2-50-21	383	50.2	10.8	0.0284	9.548	-8.29
Nd-2-50-22	428	50.1	10.1	0.0284	9.513	-8.15
Nd-2-100-1	436	100.3	12.1	0.0284	8.421	-9.14
Nd-2-100-2	452	100.2	11.7	0.0284	8.420	-9.00
Nd-2-100-3	460	100.2	16.6	0.0281	7.379	-8.53
Nd-2-100-4	476	100.2	16.3	0.0281	7.435	-8.55
Nd-2-100-5	484	100.3	15.9	0.0298	5.596	-3.33
Nd-2-100-6	500	100.3	15.6	0.0297	5.602	-3.34
Nd-2-100-7	508	100.3	15.8	0.0369	5.362	-2.63
Nd-2-100-8	524	100.3	15.3	0.0352	5.387	-2.70

Nd-2-100-9	533	100.3	15.8	0.0263	5.724	-3.72
Nd-2-100-10	554	100.3	14.8	0.0263	5.723	-3.71
Nd-2-100-11	574	100.3	14.7	0.0255	6.023	-4.56
Nd-2-100-12	596	100.2	13.1	0.0254	6.513	-5.91
Nd-2-100-13	604	100.3	12.7	0.0254	6.497	-5.76
Nd-2-150-1	619	150.1	18.2	0.0255	5.804	-5.94
Nd-2-150-2	643	150.0	16.6	0.0255	5.890	-5.88
Nd-2-150-3	651	150.1	17.1	0.0255	5.506	-4.81
Nd-2-150-4	668	150.1	15.8	0.0255	5.503	-4.83
Nd-2-150-5	676	150.1	15.6	0.0264	5.068	-3.63
Nd-2-150-6	691	150.1	15.2	0.0263	5.070	-3.66
Nd-2-150-7	722	150.1	15.1	0.0309	4.791	-2.87
Nd-2-150-8	743	150.1	14.6	0.0309	4.792	-2.87
Nd-2-290-1	764	290.1	89.6	0.0316	3.496	-2.98
Nd-2-290-2	787	290.0	89.2	0.0315	3.493	-3.00
Nd-2-290-3	796	290.1	92.2	0.0286	3.663	-3.39
Nd-2-290-4	812	290.1	93.3	0.0286	3.665	-3.41
Nd-2-290-5	820	290.1	94.1	0.0274	3.833	-3.82
Nd-2-290-6	836	290.0	93.6	0.0270	4.039	-4.28
Nd-2-290-7	839	290.0	94.6	0.0271	4.037	-4.32
Nd-2-290-8	844	290.0	95.5	0.0271	4.275	-4.77
Nd-2-290-9	860	290.1	98.7	0.0273	4.285	-4.86
Nd-3-50-1	20	50.2	10.5	0.0313	6.494	-3.26
Nd-3-50-2	27	50.1	10.4	0.0312	6.511	-3.27
Nd-3-50-3	68	50.2	11.0	0.0312	6.540	-3.27
Nd-3-50-4	77	50.1	10.8	0.0312	6.544	-3.27
Nd-3-50-5	92	50.1	14.8	0.0312	6.553	-3.27
Nd-3-100-1	100	100.3	17.6	0.0311	5.583	-3.29
Nd-3-100-2	122	100.2	15.4	0.0311	5.588	-3.30
Nd-3-150-1	164	150.1	18.1	0.0310	4.847	-3.32
Nd-3-150-2	168	150.0	17.8	0.0311	4.847	-3.32
Nd-3-290-2	196	290.1	93.9	0.0295	6.898	-7.81
Nd-3-290-3	212	290.0	95.6	0.0295	6.665	-7.67
Nd-3-290-4	220	290.1	95.7	0.0296	6.661	-7.36
Nd-3-290-5	236	290.1	98.5	0.0297	6.335	-7.30
Nd-3-290-6	244	290.1	99.5	0.0297	5.974	-7.36
Nd-3-290-8	292	290.0	105.3	0.0297	5.490	-7.06
Nd-3-290-9	316	290.0	113.0	0.0296	5.043	-6.21
Nd-3-290-10	332	290.1	114.9	0.0297	5.037	-6.61
Nd-3-290-12	365	290.0	120.8	0.0298	4.609	-5.70
Nd-3-290-13	380	290.1	124.6	0.0299	4.658	-5.83
Nd-3-290-14	388	290.1	124.2	0.0300	4.745	-6.01
Nd-3-290-15	410	290.1	126.8	0.0301	4.699	-6.01
Nd-4-50-1	28	50.2	12.7	0.1017	6.653	-3.37
Nd-4-50-2	51	50.1	12.4	0.1017	6.687	-3.38
Nd-4-50-3	124	50.1	14.4	0.1016	6.709	-3.40
Nd-4-50-4	140	50.2	14.3	0.1016	6.711	-3.40
Nd-4-100-5	148	100.3	17.6	0.1015	5.739	-3.44
Nd-4-100-6	164	100.2	17.3	0.1015	5.744	-3.44
Nd-4-100-7	172	100.2	17.1	0.1015	5.745	-3.43
Nd-4-150-8	188	150.1	22.9	0.1017	5.017	-3.46
Nd-4-150-9	196	150.0	22.6	0.1017	5.018	-3.47
Nd-4-150-10	215	150.1	22.2	0.1016	5.021	-3.48
Nd-4-200-1	222	199.8	59.7	0.1021	4.477	-3.53
Nd-4-200-2	237	200.2	59.4	0.1020	4.473	-3.55
Nd-4-200-3	245	200.1	58.5	0.1021	4.472	-3.54
Nd-4-250-1	260	250.1	86.0	0.1034	4.050	-3.61
Nd-4-250-2	284	250.1	84.1	0.1033	4.066	-3.67
Nd-4-250-3	291	250.1	83.1	0.1034	4.068	-3.67
Nd-5-290-1	22	290.0	100.9	0.1015	3.789	-3.64
Nd-5-290-2	29	290.1	100.5	0.1016	3.772	-3.62
Nd-5-290-3	46	290.0	103.1	0.1012	4.178	-4.63
Nd-5-290-4	54	290.0	102.5	0.1013	4.352	-5.00

Nd-5-290-5	70	290.1	102.2	0.1014	4.544	-5.51
Nd-5-290-6	77	290.0	101.4	0.1015	4.701	-5.69
Nd-5-290-7	105	290.0	102.3	0.1017	4.958	-6.08
Nd-5-290-8	128	290.0	106.3	0.1019	5.221	-6.39
Nd-5-290-9	166	290.0	124.0	0.0974	3.406	-2.97
Nd-5-290-10	173	290.0	124.1	0.0975	3.406	-2.97
Nd-5-290-11	190	289.0	130.3	0.0970	3.517	-3.29
Nd-6-50-1	21	50.2	14.0	1.0085	6.681	-3.55
Nd-6-50-2	27	50.1	13.7	1.0084	6.734	-3.56
Nd-6-50-3	45	50.2	13.6	1.0084	6.793	-3.58
Nd-6-50-4	72	50.2	13.3	1.0083	6.809	-3.59
Nd-6-100-1	93	100.3	16.3	1.0085	5.857	-3.64
Nd-6-100-2	99	100.2	16.1	1.0085	5.859	-3.64
Nd-6-150-1	116	150.1	21.8	1.0112	5.139	-3.70
Nd-6-150-2	124	150.0	21.5	1.0113	5.141	-3.71
Nd-6-200-1	140	200.1	33.7	1.0184	4.558	-3.73
Nd-6-200-2	146	200.1	33.3	1.0189	4.560	-3.75
Nd-6-250-1	164	250.1	58.2	1.0349	4.180	-3.94
Nd-6-250-2	172	250.1	57.8	1.0363	4.182	-3.95